Measurement of Surface Tensions in Aggregated Cells of the Embryonic Chick

By Jen Sweny

A thesis
presented to the University of Waterloo
in fulfillment of the
thesis requirement for the degree of
Master of Science
in
Biology

Waterloo, Ontario, Canada, 2007

I hereby declare that I am the sole author of this thesis. This is a true copy of the thesis, including any required revisions, as accepted by my examiners. I understand that my thesis may be made electronically available to the public.

Abstract

Cell surface properties are crucial to the mechanisms by which groups of cells organize themselves during embryogenesis, cancer metastases and tissue engineering. Measured surface tension values provide a quantitative basis for predicting a range of cell behaviors including sorting of embryonic cells, self-organization of pancreatic islet cells and invasive potential of tumor cells. Tissue surface tensions are a measurement of the tension that acts along the interface between a cell aggregate and its surrounding media and it is typically measured by compressing an aggregate of cells. In this study a novel apparatus is used to measure the surface tensions of aggregated embryonic chick cells from heart, liver, neural retina and mesencephalon tissues. These surface tension values are consistent with the known engulfment behavior of the cells involved and are in close agreement with measurements made previously by other means. It has been suggested that surface tensions and cell rearrangement patterns are a direct result of adhesion forces between cells arising from cadherins. However, cadherin binding alone is insufficient to account for observed engulfment phenomena and recent experimental evidence suggests that actin dynamics are involved. A cell surface property referred to as interfacial tension or cortical tension takes into account both adhesion forces and forces derived from actin microfilaments and could shed new light on the mechanisms involved in cell interactions. Computer simulations indicate that the interfacial tension between cells can be measured through a modified compression test experiment. In this cell aggregate compression study, cell shapes as well as the aggregate profile are measured in addition to the compression force in attempts to measure cell interfacial tensions.

Acknowledgements

I would first like to thank my supervisor, Dr. G. Wayne Brodland for giving me the opportunity to work on this project and providing his support and guidance. His knowledge and expertise were greatly appreciated.

I would also like to thank my committee members Bruce Reed and Niels Bols for their input and time. As well I would like to especially thank Dr. Reed for the use of his fruit flies while we were developing the equipment.

Thanks go as well to Caleb Horst and Paul Groh for help with apparatus design, for putting together the equipment and for always being around to troubleshoot when I had problems. I would also like thank Jim Veldhuis for the design of the software used in this project and Abby for her help proofreading this thesis.

In addition I would like to thank all the members of the Brodland lab over the years. From the camping trip we took on my first day of work, to all the amazing potlucks, mountain biking and other fun outdoor trips it has been a great time. Specific thanks to Richard Benko for getting me started in the lab and countless hours of entertaining conversation, to Jim and Caleb for making excellent lunchtime mountain bike partners, and finally to Fatima, Abby and more recently Paul and Simon for their company in the lab.

Outside of the lab I would like to thank my friends and family for their support. Mom and Dad for their support and a home cooked meal every now and again. Andrea for her excellent extended visits, Chris and Loren for the great mid-degree vacation in Alaska, Ryan and Justyna for the fun trips back to Ottawa, and to Neal Ross-Ross for help with my debating skills and for his daily questions regarding whether I am done writing yet.

Table of Contents

List of Figures

List of Tables

List of Equations

Equation 1: $\sigma(1/R_1 + 1/R_2) + P_{ext} = \lambda$

$$\frac{N}{m}(\frac{1}{m} + \frac{1}{m}) + \frac{N}{m^2} \sim \frac{N}{m^2}$$

Equation 2: $$\sigma = \frac{F}{\pi R_3{}^2 (1/R_1 + 1/R_2)}$$

$$\frac{N}{m} \sim \frac{N}{m^2(\frac{1}{m} + \frac{1}{m})}$$

Equation 3: $F_{cyto\,2D} = 4\mu R_3 \dot{\varepsilon}$

$$\frac{N}{m} \sim \frac{N \bullet s}{m^2} \bullet m \bullet \frac{1}{s}$$

Equation 4: $F_{cyto3D} = 3\pi\mu R_3{}^2 \dot{H} \Big/ H$

$$N \sim \frac{N \bullet s}{m^2} \bullet m^2 \bullet \frac{m \Big/ s}{m}$$

Equation 5: $F_{CM} = \pi\gamma_{CM} R_3{}^2 (1/R_1 + 1/R_2)$

$$N \sim \frac{N}{m} \bullet m^2(\frac{1}{m} + \frac{1}{m})$$

Equation 6: $F_{CC} = \pi R_3{}^2 (\sigma^{\gamma}{}_r - \sigma^{\gamma}{}_z)$

$$N \sim m^2(\frac{N}{m^2} - \frac{N}{m^2})$$

Equation 7: $\sigma_r^{\gamma} = \gamma_{cc} f_r^{\gamma}$

$\sigma_z^{\gamma} = \gamma_{cc} f_z^{\gamma}$

$$\frac{N}{m^2} \sim \frac{N}{m} \bullet \frac{1}{m}$$

Chapter 1 Introduction

1.1 General Introduction

Recent research has shown that cell surface properties are crucial to the mechanisms by which cells organize themselves during embryogenesis, cancer metastases, and tissue engineering. This thesis concerns the quantitative characterization of these surface properties through the measurement of cell aggregate surface tensions and cell-cell interfacial tensions.

In liquids the molecules in the bulk of the liquid are equilibrated by cohesive Van der Waals forces from surrounding molecules. However, at the surface of a liquid, molecules are subjected to an imbalanced force that pushes them away from the surface and creates surface tension. The cost in energy for a change in the liquid surface area is directly related to the surface tension (1). The term surface tension applies to the situation where a liquid-gas interface is involved, while when a liquid adjoins another liquid or a solid the tension is referred to as an interfacial tension (1).

Cells in a tissue behave in many ways like liquids and mixtures of heterotypic cells often behave like immiscible liquids. In cellular systems the subunits are cells rather than molecules and the surface tension refers to the tension acting at a cell-medium interface while, interfacial tension refers to the tension acting at a cell-cell interface (2). It is important to distinguish between these terms as they are separate properties and are measured using different techniques.

The measurement of surface tension provides insight into how a wide range of developmental and tissue-forming events occur as well as providing a way to measure the invasive potential of tumor cells. Surface tension of various tissues including embryonic chick tissues (2-4), pancreatic islet cells (5), fibrocarcinomas (6), lung tumors (7), and brain tumors (8) have been measured and proven useful in predicting the sorting behavior between populations of cells. In surface tension measurement experiments the tension

between growth medium and an aggregate of cells is measured under physiological conditions and involves the compression of an aggregate between parallel plates.

It has been shown that the relative surface tensions between two groups of cells dictate that those with the lesser surface tension will surround those with the higher one (9). It has also been suggested that surface tensions and sorting behavior are governed solely by adhesion arising from cadherin interactions between cells (5, 10). However, recent research has shown that binding between cadherin molecules alone are not sufficient to account for sorting behavior and the role of actin dynamics in cell interactions has been re-emphasized (1, 11, 12). In addition, surface tension forces depend on the ability of the lipid bilayer to increase its surface area in response to myosin molecular motors acting on actin filaments (1). The dynamics of cell-to-cell contacts involve an interplay between adhesion which increases cell contact area and another property referred to as cortical tension (1) or interfacial tension (13) which shortens the cell-cell boundary. Interfacial tension as described by Brodland (13), refers to the net tension that acts along the boundaries of cells. It takes into account forces derived from adhesion, as well as those derived from the cytoskelatal components and actin dynamics (13, 14). The measurement of this property could provide the information needed to verify this comprehensive framework for cell sorting.

Computer simulations have shown that interfacial tensions may be measured using cell aggregate compression tests similar to those used to measure surface tension (15). To obtain the surface tension of an aggregate of cells, the aggregate profile must be monitored in addition to the force required to compress the aggregate. The forces involved are quite small and the instruments used to measure them must be very precise. An apparatus that can compress the aggregate while monitoring the force required to do so and the shape of the aggregate requires both mechanical and microscopy components to work together in conjunction with the software used to control the devices. In addition to these components the calculation of interfacial tension requires that the geometry of the cells within the aggregate be visible as it is compressed. Visualizing the cells within

an aggregate requires high powered objective lenses, confocal microscopy abilities and fluorescent labeling techniques.

The present study uses a novel apparatus to measure surface tension in aggregated cells from embryonic chick tissue. In addition this device is used to monitor cell shapes as an aggregate is compressed in order to verify the mechanics of the interfacial tension theory.

1.2 Overview of Thesis

The present thesis comprises five chapters. In this chapter the method for measuring tissue surface tension and interfacial tensions are introduced, the relationship between the two properties, and the importance of these values in understanding cell behavior are established. Chapter 1 also contains an overview of the thesis. Chapter 2 reviews previous studies on the measurement of cell surface tension, background on cell interfacial tensions and the importance of cell interactions. Chapter 3 describes experiments involving the measurement of surface tensions of embryonic chick cell aggregates. Surface tension results are discussed with respect to those obtained by other groups and a validation test of the measurement of the surface tension of water is discussed. Chapter 4 details the steps taken to measure interfacial tension and the results of these experiments. Chapter 5 discusses other applications for the compression device and future directions of the research.

Chapter 2 Review of Literature

2.1 Cell Interactions

Understanding how cells interact and form tissues is important to many applications including embryo development (16-18), cancer metastasis (8, 19-22), tissue formation (5), tissue engineering (23-25, 25), and regenerative medicine (26-28). Computational models of cell interactions provide a complement to experiments and in order for useful information to be gathered from them the models must use accurate parameters for the cell interactions (23, 29-32). This section discusses how cell interactions are relevant to the above fields.

2.1.1 Cell Interactions in Embryo Development

As an embryo develops germ layers segregate and newly formed tissues move over each other and the extracellular matrix to rearrange and eventually take up their characteristic body plan (20). Rearrangements are seen during the processes of gastrulation, neurulation and organogenesis and separation of cell types occurs constantly during embryo development (2)

The physical properties of embryonic cells are central to understanding how these rearrangements take place. Although progress has been made the physical mechanisms which cells use to change position as well as the forces within the embryo which affect these movements are still poorly understood (33). From a molecular perspective, the interactions of cells with each other and the extracellular matrix (ECM) are mediated by cadherins, integrins, and proteases including matrix metalloproteinases (34). Actin, which is involved in cytoskeletal contractibility is also involved in cell interactions as it plays a role in cell migration (35) and cell shape changes (1, 35) as well as interfacial tension (1, 13).

2.1.2 Cell Interactions in Cancer Metastasis

Tumor growth and embryo development share the common requirement of cell proliferation and cell differentiation. Adhesion molecules including cadherins and integrins are involved in the transition of organ-confined tumors to invasive malignancies (7). When tumor cells become malignant boundaries and compartments are disassembled and the tumor cells become miscible in the tissue they are invading (20). Whether tumor cells segregate or intermix depends in part on a balance between the forces binding cells together and those promoting interaction of tumor cells with various components of their environment (20). When a cell becomes invasive, it acquires the ability to detach from the tumor mass, a process which requires some degree of affinity for the stroma in which it resides. The measurement of strength of cell interactions via surface tension measurements have been correlated inversely with the invasive potential of lung tumors, fibrosarcomas and brain tumors (5, 36). In addition cadherin expression has shown to be involved in the elimination of tissue boundaries in brain, breast and prostate cancer (9, 22).

2.1.3 Cell Interactions in Tissue Formation

Cell interactions and sorting patterns play a role in how certain tissues for example the islets of Langerhan are formed (5). The organization of endocrine cells in pancreatic islets occurs through a series of cell sorting, migration and aggregation events, where one type of cell, the insulin producing beta-cells form the core while several other types of cells including glucagons, somatstatin and pancreatic polypeptide-producing cells segregate to the periphery. Isolated pancreatic islet cells have the ability to self-assemble in vitro into the same arrangement as in native islets (5). Surface tension measurement experiments using immortalized rodent pancreatic islet cells showed that the internal beta-cells had lower surface tension values than the other islet cells which engulf or surround them. This result shows that the interaction between the two cell types could be predicted through the measurement of their surface tensions.

2.1.4 Cell Interactions in Tissue Engineering and Regenerative Medicine

Tissue engineering is an interdisciplinary field that seeks to provide a new solution to tissue loss by replacing lost or diseased tissue. Constructs that contain specific populations of cells in specific geometries have been designed (27). Tissues which have been engineered to display functional characteristics include: beating cardiomyoctye spheroids, liver-like hepatocyte spheroids, human umbilical vein endothelial cells with the ability to vascularize fibroblast aggregates, and dorsal root ganglion cells with the ability to extent ganglion-like projectsion into fibroblast aggregates. Other larger structures have been tissue engineered including skin and blood vessels (24).

The design of tissues involves prediction of both cell-cell interactions and interactions of cells with the scaffold (24) and it is the self-assembling properties of cells which allow for these predictions to be made (28). The type of cell, type of material used as a scaffold and the design of the scaffold can all be adjusted to obtain structures with the desired characteristics. Designed structures range from simple tube structures formed by places aggregates along the edge of a circle (23) to lumenized tubes and thick cellular sheets (37).

2.1.5 Modeling of Cell Interactions

Computer simulations have been used to model how cells interact during embryo development and can provide a useful tool in determining how various factors affect cell surface properties and processes related to these properties (38, 39). Many studies have been performed using computer models to gain insight into properties of cells and embryos (23, 29-32)(14, 15). There are several approaches used to model cell interactions including cell and sub-cellular lattices, body centric, boundary vertex and finite element models (14) which have been used to gain valuable insight into the mechanisms of cell interactions.

Modeling has been a valuable tool in several types of experiments including tissue engineering experiments where modeling was used to predict the final structure of aggregates placed in close proximity to each other (23), cell movement and sorting

experiments where the movement of cells in response to adhesive forces were modeled and accurately predicted behavior of dissociated cell population as well as interactions between multiple populations (29). Several methods of modeling were used for cell sorting predictions, one used self-population and cross population adhesive bonds (29) while another model used the potential energy associated with the mutual interaction between the cells to derive the energy of interaction of biological cells (32).

Computer models have also been used to analyze surface tension measurements in new ways. Compression tests used to measure surface tension of an aggregate of cells were analyzed using a finite element analysis and new information was determined from them (14). It was determined that the resistance to compression of the aggregate was a result of viscosity of the cytoplasm, tension between the aggregate and the medium and tension between cells within the aggregate. It was previously thought that surface tensions were strictly a result of adhesion forces and this computer simulation was one of the first of several studies to indicate that other factors were involved. In addition, models can be used to suggest new experimental approaches. A similar model done in three dimensions where cells were assumed to be polyhedral in geometry and have a constant tension acting along the cell-cell interfaces was used to predict sorting and envelope behaviors for aggregates of up to a hundred cells (15). This model took into account both surface tension, interfacial tension and the viscosity of cells and accurately predicted cell behaviors in three dimensions.

2.2 Mechanics of Cell Interactions

2.2.1 Cellular Components Involved in Cell Surface Properties

Cellular components give rise to surface tensions, which give rise to local interactions, which in turn result in cell and tissue motion. The surface properties of a cell are a result of many cellular components. The lipid membrane and the channels, receptors and adhesion molecules it contains allow for the chemical balance and electronegativity of the cell to be maintained, for the cell to communicate with adjacent cells, to sense deformation and to transmit forces from one cell to another. The

endoplasmic reticulum, golgi apparatus, perioxisomes and lysosomes are a part of the membrane system and are recycled to the membrane through exocytosis and endocytosis (14). Cell adhesion molecules (CAMs) found in the lipid membrane bind to each other, extracellular matrix, and to various substrates. Cell-cell adhesions and cell-substrate adhesions can be classified as either homotypic, if two of the same CAMs are involved or heterotypic if two different types of CAM are involved (1). CAMs generate a constant amount of force per unit of cell contact area (14) of a magnitude that varies based on the cell type involved (14) and the associated CAMs which are involved (12). The force generated through adhesion acts in a direction that is tangential to the cell-cell interface and tends to lengthen the boundary which it is acting on. The membrane and its associated structures vary between cell types and give rise to a tension that acts in the plane of the membrane as well as cause viscoelastic, tensile and bending properties (14). The tension that results from the membrane is opposite in direction to the adhesion force derived from CAMs.

Cytoskeletal components including microfilaments, intermediate filaments and microtubules maintain the cell's shape. The state of the cytoskeleton is dependant on the environment of the cell; and when cells are in an aggregate actin microfilaments tend to organize themselves along the inside edges of cells creating a force that is parallel to that of the cell surface. When a cell is exposed to its surrounding media there is an increase in microfilaments along that edge and an increase in surface contraction. The cell's cytoplasm generates a hydrostatic pressure that balances the tension produced along the cell surfaces to maintain the volume of each cell (14). A schematic diagram of the cell showing the cytoskeletal and membrane bound components of a cell is shown in Figure 2.1.

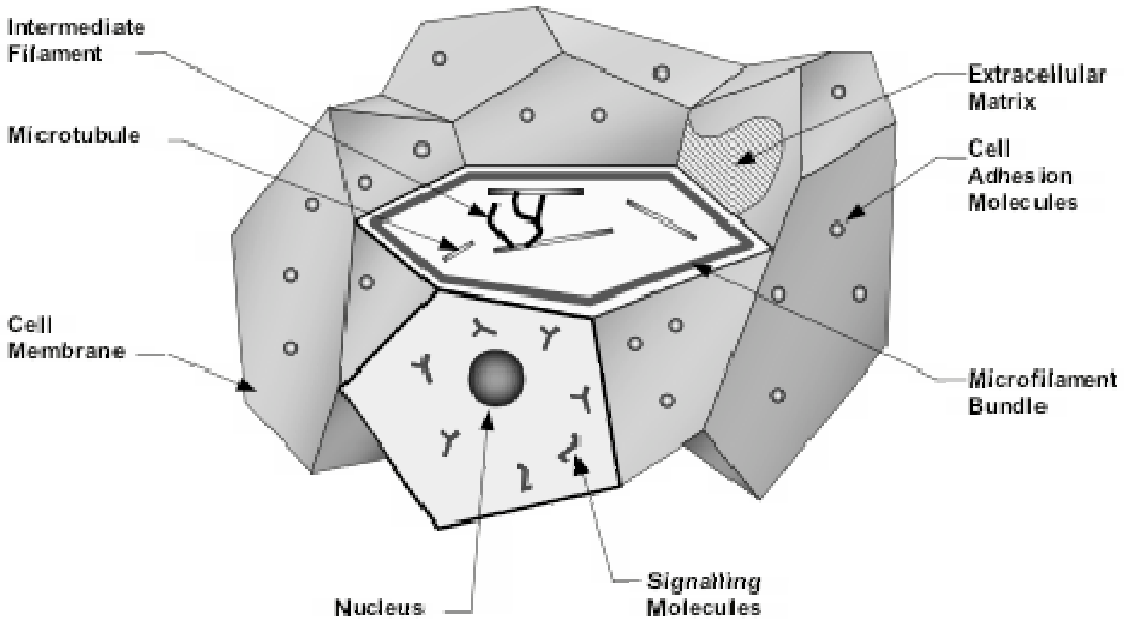

Figure 2.1: Schematic of cells within an aggregate. The forward-most cell has been sectioned to show the nucleus and signaling molecules inside the cell, as well as microtubules and intermediate filaments within the cytoplasm, and microfilaments along the top inner surface. Also shown are the extracellular matrix and cell adhesion molecules between cells. From Brodland (14)

2.2.2 Mechanics of Cells in Aggregates

At cell-cell contact areas the tension between cells results in local interactions between those cells. The net tension referred to as interfacial tension (γ) is a result of the interplay between cell adhesion and the tension acting parallel to the cell interface (1, 12). In an aggregate of cells there are interfacial tensions acting between cells within the aggregate and surface tension acting where the cells within the aggregate are in contact with their surrounding media. In the case that an aggregate has cells of different types several interactions can occur based on the strength of the interfacial tensions between the cells and the surface tensions between cells and their surrounding media (12). In Figure 2.2 cell junctions between two types of cell and between a single type of cell and media are shown. In addition two cell patterns that arise based on tensions between cells within an aggregate are shown. When two types of cells are intermixed they either sort or mix. Cells will mix when the interfacial tensions between two cells of the same type are significantly stronger than then tensions between two different types. Cells will sort when the tension between two cells of different type is significantly stronger than the interfacial tensions between cells of the same type. The differences in interfacial tensions result in local movement of the cells with respect to each other and over time sorting and mixing patterns result.

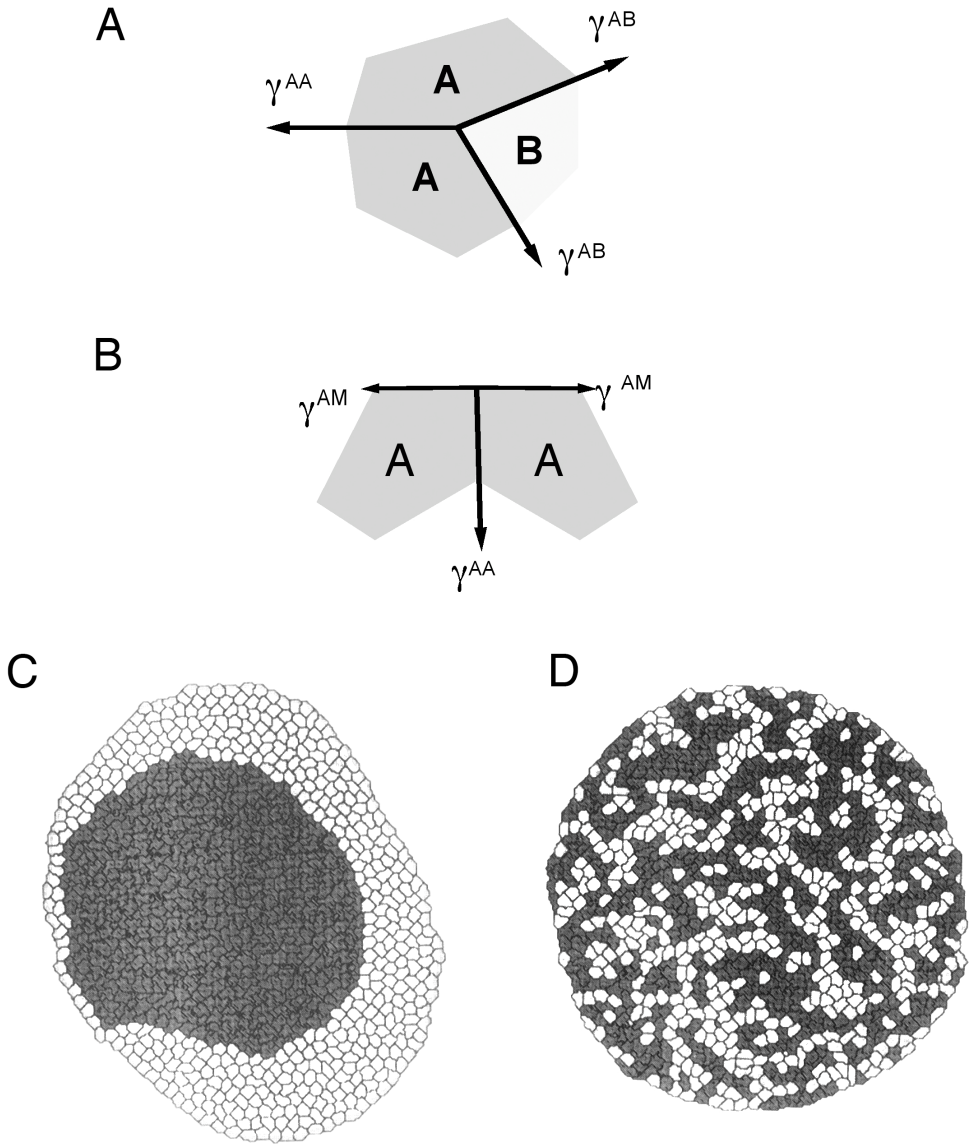

Figure 2.2: Interfacial tension and surface tension resulting in sorting and mixing behaviors. (A) shows the interfacial tension acting between two type A cells and one type B cell. (B) shows the interfacial tension acting between two type A cells and their surrounding media. (C) shows a case where the interfacial tensions between the dark and light cells is significantly greater than those of the light cells with each other and the dark cells with each other and sorting results. (D) shows a case where the tensions between dark and light cells is significantly less than the tension between cells of the same type and mixing occurs. From Brodland (14).

2.3 Theories Regarding Cell Interactions

Embryonic cells were initially used in experiments as a result of their unique liquid-like properties. Several theories have attempted to explain these properties and are discussed in this section:

2.3.1 Study of Embryonic Cells

Embryonic cells initially became of interest when experiments done by Johannes Holtfreter in 1939 showed that pieces of amphibian embryonic tissue had behaviors typically associated with liquids. In Holtfreter's experiments embryonic tissues were shown to round up when isolated *in vitro*. In addition, they adhered to and spread over each other in specific configurations. He also found that certain tissues showed what he called affinity for each other while others avoided association. In subsequent involving embryonic tissue dissociated into single cells, Holtfreter found embryonic tissue possessed the ability to self-arrange and sort into distinct layers based on its origin (40). This self-arrangement was said to be governed by "tissue affinity" and became a key subject of interest to researchers studying morphogenesis.

Subsequent studies showed the same sorting behaviors in embryonic cells from mammals, birds, and insects (41, 42). Researchers then became interested in the mechanisms that caused embryonic cells to sort and studies showed that when two cell types mixed several intermediate arrangements were observed (43). These cell arrangements included partial engulfment, linking and checkerboard patterns and are diagrammed in Figure 2.3. Possible explanations for the behavior of embryonic cells during sorting and engulfment was the source of much theoretical speculation and led to several hypotheses regarding cell behavior.

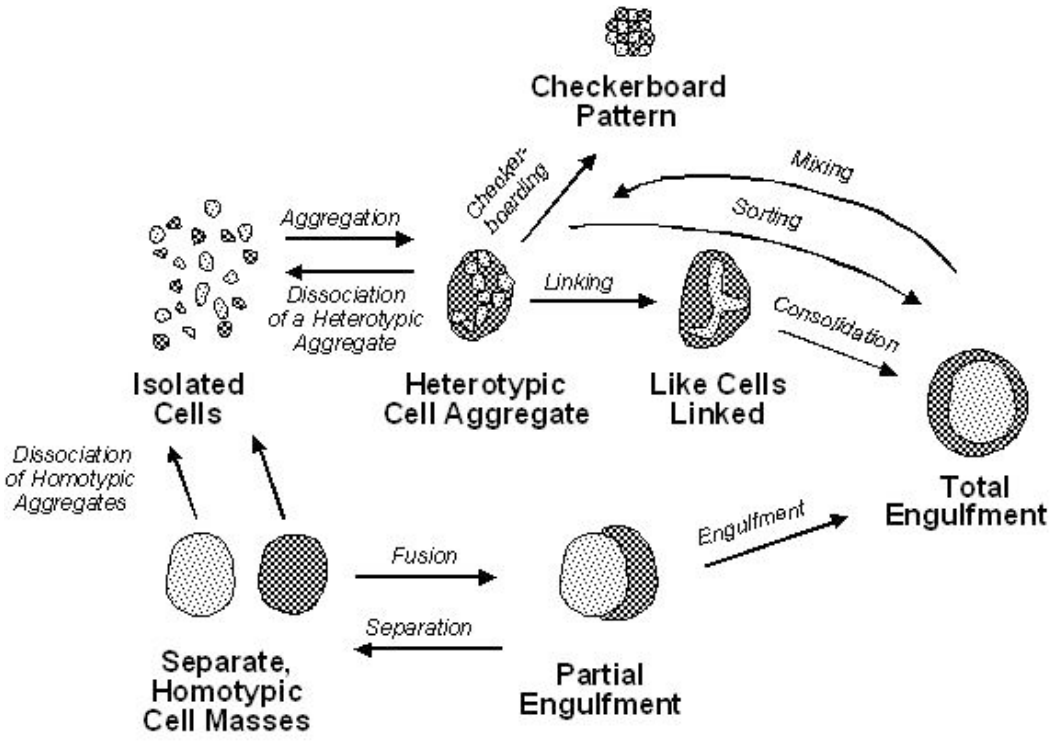

Figure 2.3: Behaviors of embryonic cells. Depending on the properties of cells, many behaviors can occur when two cell types contact each other. These include fusing with partial or complete engulfment, aggregation, and sorting to produce engulfment or a checkerboard pattern. From Brodland (14).

2.3.2 Explanation for Embryonic Cell Behavior

Several theories regarding the sorting of cells have been put forth since the initial experiments performed by Holtfreter. Holtfreter himself suggested that the behavior was a result of chemotaxis and selective adhesion (40). Other groups who were studying cell sorting attributed the sorting behaviour to differential (43) or specific (42) adhesion.

The first proposed hypothesis and also the most widely accepted is the differential adhesion hypothesis (DAH) which was first presented by Steinberg in 1963 (43). It states that the liquid-like tissue-spreading and cell segregation events of development arise from tissue surface tensions which in turn arise from differences in intercellular adhesiveness. This hypothesis was challenged by numerous research groups (44, 45) and subsequently alternative hypotheses were formed. First, the differential surface contraction hypothesis (DSCH) was proposed in 1976 by Harris (45). This hypothesis was based on surface contractions of cells, which were thought to be greatest when a cell was in contact with the media, less when it contacts a cell of a different type, and least when a cell was in contact with another cell of the same type.

Although largely unchallenged for 40 years, computer simulations showed that the DAH failed to explain key aspects of tissue sorting and engulfment. Another theory, based on computer simulations and analytical calculations called the Differential Interfacial Tension Hypothesis (DITH) was developed in 2002. The DITH explains the sorting and spreading behaviors of embryonic cells based on differences in interfacial tensions between cell types (13). Interfacial tension is the tension that acts on the boundary between cells and is a result of cell-cell adhesion as well as contributions from actin dynamics and the cell cytoskeleton. The DAH has failed to explain certain properties of embryonic cells. Experiments performed by Wisemen showed populations of less cohesive cells migrating into subsurface positions of cell aggregates made up of more cohesive cells (44), a result that is consistent with DITH. Whereas, DAH predicts that populations of less cohesive cells would not be able to migrate into a more cohesive mass and computer simulations based on the DAH principles showed that in general, cells will not penetrate a tissue mass composed of cells more cohesive than themselves

(44). This work indicates that aspects of the DAH need to be changed for it to accurately predict embryonic cell behavior. Another postulate of the DAH is that tissue surface tensions that underlie tissue segregation, spreading, and sorting are generated purely from the intensities of adhesion between cells. This aspect of the hypothesis has been tested using cell lines with various types of cadherins as the only adhesion molecule (10), implying that other molecules do not contribute to changes in cell surface tension. However, evidence has shown that the surface tension of a cell depends on the state of its cytoskeleton (1, 46, 47) and actin dynamics within the cell (1) and that cell sorting by cadherin adhesion must be determined by mechanisms other than selective homophilic cadherin interactions (12).

The difference between interfacial tension and adhesion is shown in Figure 2.4. Interfacial tension shortens the length of the interface on which it acts and a cell-cell adhesion increases the length of the boundary on which it acts (30). Actin filaments act along the edge of each cell and generate a contractile force, while cell adhesion forces elongate the interface between the two cells releasing energy as the new contact is formed (13).

Cell-cell adhesion and interfacial tensions can act simultaneously even though they would be opposing each other. The net interfacial tension includes the effect of cell-cell adhesion (48). In order to determine whether strictly adhesion or interfacial tension results in the behaviors exhibited, interfacial tensions between cells must be measured. Determining the experimental interfacial tension will allow a comparison to be made between the calculated interfacial tension and the measured value. If the values match closely this would provide evidence that interfacial tension is the governing factor in cell interactions rather than adhesion.

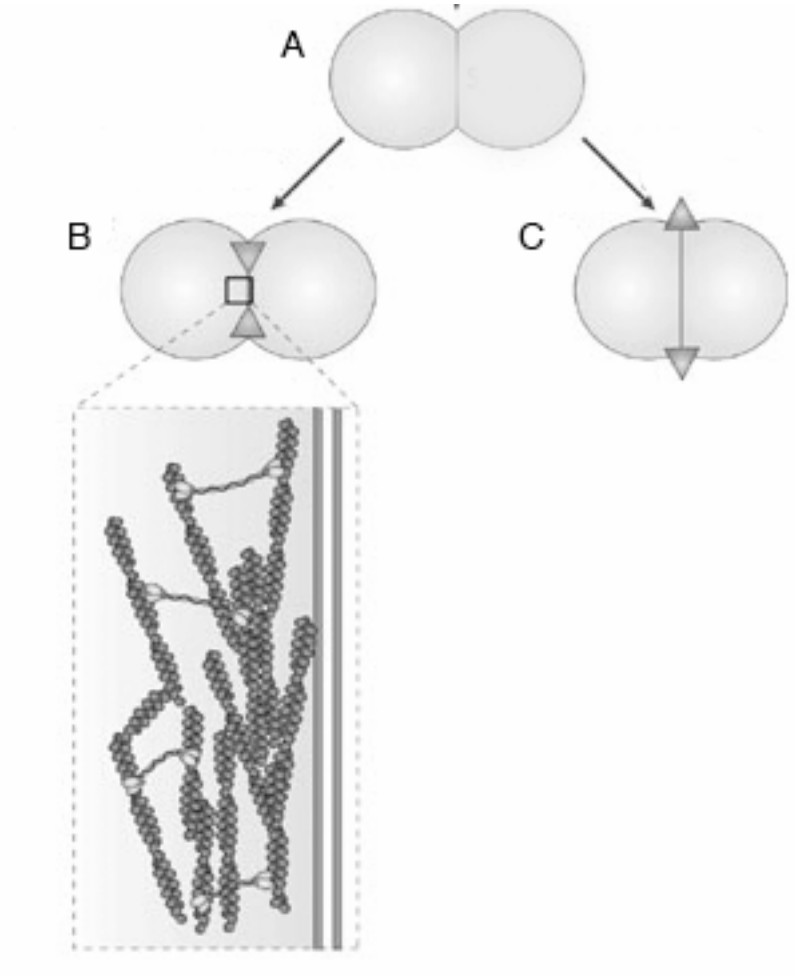

Figure 2.4: Cell adhesion and cell interfacial tension. Cells in contact with each other (A) are acted on by both cell interfacial tension (B) which lengthens the contact boundary and cell adhesion (C) which shortens the contact boundary. Cell adhesions are a result of cadherins while cell interfacial tension are a result of the acto-mysosin network. From Lecuit (1).

2.4 Aggregate Compression Tests

2.4.1 Liquid-Like Behavior of Tissues

Embryonic tissue, as well as several other types of tissue display behavior similar to that of liquids. Liquids are regarded as a population of mobile cohesive subunits. In water the subunits would be individual water molecules while in tissues the subunits would be individual cells. If you have 2 liquids (a and b) where one has a surface tension of $\sigma_{a,}$ the other has a surface tension of σ_b and σ_{ab} is the surface tension between them, the two liquids will be immiscible if σ_{ab} is greater than zero and if σ_a is greater than σ_b then liquid b will spread over liquid a . This relationship is transitive and has been shown to apply to numerous embryonic tissues (2) as well as other tissues including tumor cell lines and pancreatic islets (5). For a tissue to be considered liquid-like it must display the following characteristics: aggregates must form spheres and aggregate cohesivity must be independent of the applied force and aggregate size.

2.4.2 Compression of Embryonic Tissue

The Laplace equation is commonly used to determine the surface tension of a liquid droplet compressed between parallel plates to which it does not adhere. The equation is:

$$\sigma(1/R_1 + 1/R_2) + P_{ext} = \lambda \qquad [1]$$

$$\frac{N}{m}\left(\frac{1}{m} + \frac{1}{m}\right) + \frac{N}{m^2} \sim \frac{N}{m^2}$$

where P_{ext} is the external pressure acting on the droplet's surface, σ is the interfacial tension between the droplet and the surrounding media, and R_1 and R_2 are the two principal radii of curvature of the droplet's surface shown in Figure 2.5. The Lagrange multiplier λ is a constant which is used to assure the incompressibility of the aggregate (2). This equation would be a complicated differential but it can be simplified due to the following assumed properties of the aggregates: they are spherical before compression, are axi-symmetric after compression and the side boundaries can be approximated by spherical caps. In this case $\lambda = F/\pi R_3^2$, where F is the measured weight loss on the upper compression plate and R_3 is the polar radius.

At a point at the edge the aggregate $P_{ext} = 0$ and the simplified Laplace equation for these conditions becomes

$$\sigma = \frac{F}{\pi R_3{}^2 (1/R_1 + 1/R_2)} \qquad [2]$$

$$\frac{N}{m} \sim \frac{N}{m^2 (\frac{1}{m} + \frac{1}{m})}$$

(2). To obtain surface tension of a cell aggregate the radii of curvature, and the measured changes in force on the compression plate need to be measured for each aggregate. A schematic diagram of the radii of curvature is shown in Figure 2.5.

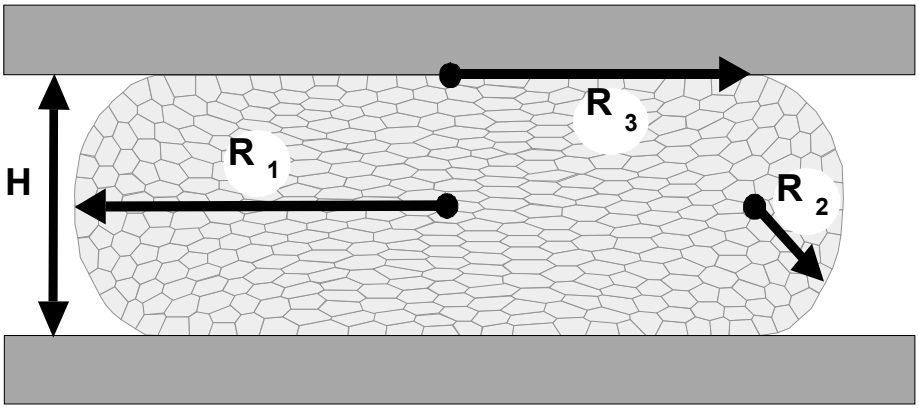

Figure 2.5: Aggregate radii of curvature used in Equation 2: R_1 and R_2 are the principal radii of curvature and R_3 is the radius of either of the contact areas between the plate and aggregate, H is the height between them. From Brodland (30).

Using a compression apparatus surface tension measurements for various types of tissues have been obtained. The initial apparatus used by Foty in 1994 had parallel plates to continuously record the force applied to a cell aggregate and the aggregate's profile shape, which was used to obtain the necessary radii of curvature (2). A schematic diagram is shown in Figure 2.6.

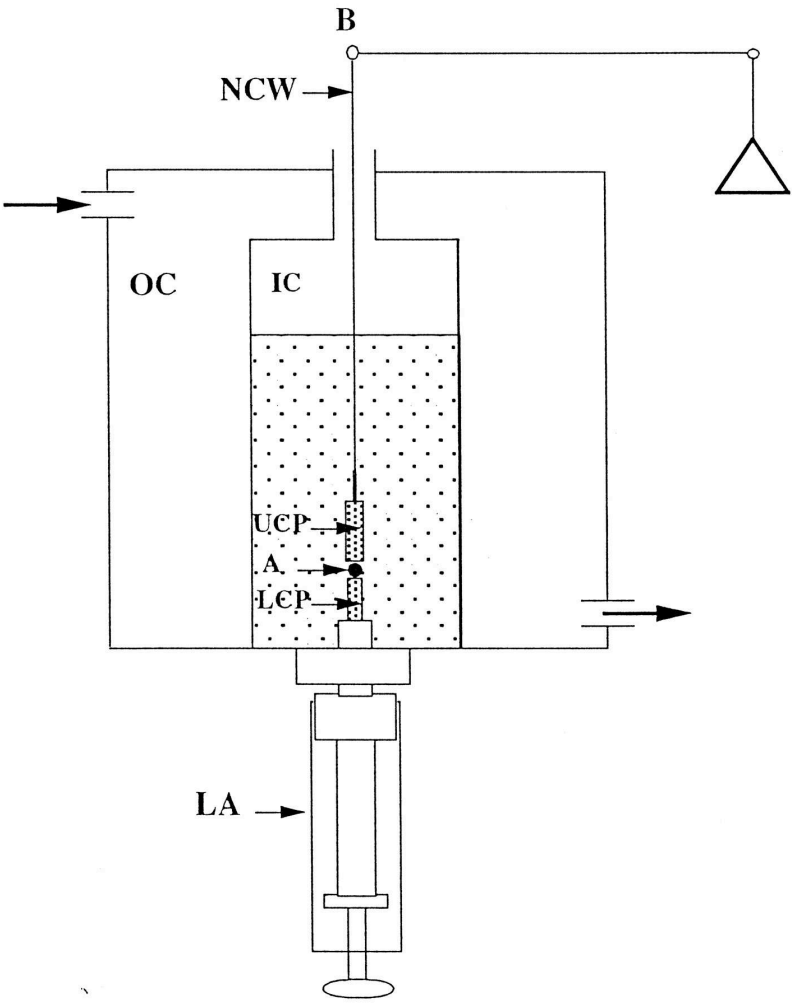

Figure 2.6: Parallel plate compression device. The apparatus contains inner and outer rectangular chambers. The outer chamber (OC) is connected to a temperature controlled circulating water pump and serves to regulate the temperature of the inner chamber (IC). The lower assembly (LA) screws into the base of the inner chamber. The position of its central core whose tip is the lower compression plate (LCP), can be adjusted vertically by a screw thread to set the distance between the two plates. The upper compression plate (UCP) is a cylinder about 15 mm long suspended from the arm of a Cahn/Ventron recording electrobalance (B) by a 0.15 mm diameter nickel-chromium wire (NCW). Its position can be adjusted horizontally to place the UCP directly above the LCP. During an experiment, a spheroidal cell aggregate (A) is positioned on the lower plate and raised until it contacts the upper plate. Compression of the aggregate reduces the load measured by the balance by an amount equal to the force acting upon the cell aggregate. From Foty (3).

2.5 Information from Force-Time Compression Data

Additional information from these tests can be gained if the shapes of cells are known. Using finite element simulations it has been determined that three mechanisms result in the generation of the force that resists compression: interfacial tension γ_{cc}, surface tension γ_{cm} (referred to as σ in above equations above), and viscous deformation of the cytoplasm (30).

2.5.1 Force Time Curves

A typical force time curve for a compression is shown in Figure 2.7. During compression the force increases until it reaches B_1. The increase corresponds to increased contact area between the cell mass and compression plates and is a result of the deformation of the cell. Once the compression stops (point B_2) only surface tension (γ_{cm}) and interfacial tension (γ_{cc}) are contributing to the net force. At point C the cells have annealed and the force acting on the plate is due to surface tension (γ_{cm}) alone. The force contributed by interfacial tension (γ_{cc}) decreases with time and accounts for the force decreases between B_2 and C (30). After the initial compression (point B_2) cells are elongated. Over time the elongated cells round up and as a result the force they exert decays until point C where cells have completely rounded up. The typical time course measured in compression tests is one to two minutes (3).

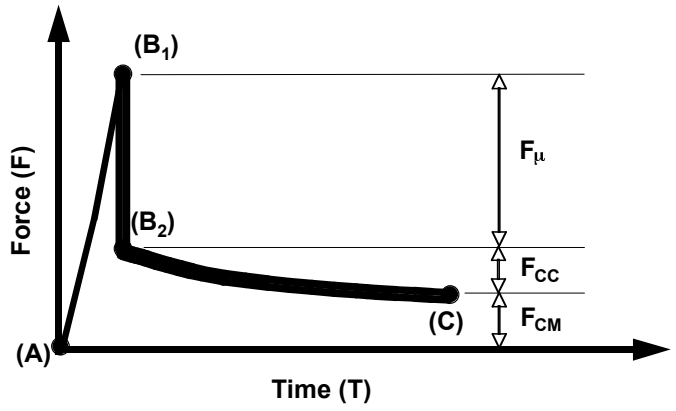

Figure 2.7: Force-time curve for compression of aggregate: B1 is the point where the force reaches a maximum due to the increased contact area between the cell mass and compression plates. At B2 the compression has stopped and only surface tension (γ_{cm}) and interfacial tension (γ_{cc}) are contributing to the force. The difference between B1 and B2 corresponds to the force contributed by cytoplasmic deformation. At point C the cells have annealed the force acting on the plate is due to surface tension (γ_{cm}) alone. The force decreased between B2 and C and this decrease in force corresponds to the interfacial tension (γ_{cc}). From Brodland (30).

2.5.2 Calculating Cytoplasm Viscosity, Surface Tension and Interfacial Tension

A two-dimensional analysis of the forces acting during the compression of a cell aggregate has been carried out and equations for viscosity (μ) and interfacial tension (γ_{cc}) have been determined. The viscosity of the cell cytoplasm can be determined via the equation:

$$F_{cyto\,2D} = 4\mu R_3 \dot{\varepsilon} \qquad [3]$$

$$\frac{N}{m} \sim \frac{N \bullet s}{m^2} \bullet m \bullet \frac{1}{s}$$

In this equation μ is the viscosity of the cytoplasm, $\dot{\varepsilon}$ is the strain rate of the compression, and F_{cyto2D} is the force produced by the bulk deformation of the cytoplasm per unit of specimen thickness as measured into the plane of the paper in Figure 2.5 . R_3 is half the contact length between the aggregate and the compression plate (30).

In a three dimensional aggregate the contribution of surface, tension, interfacial tension and cytoplasm viscosity to the total force on the plate can be calculated using the measured values during a compression test via the following formulas (derived by Brodland, unpublished):

The contribution of cytoplasm viscosity to the platen load has been determined to be:

$$F_{cyto3D} = 3\pi\mu R_3^{\,2}\, \dot{H} \Big/ H \qquad [4]$$

$$N \sim \frac{N \bullet s}{m^2} \bullet m^2 \bullet \frac{m \big/ s}{m}$$

Where R_3 is the radius of either of the contact areas between the plate and aggregate, H is the height between them and $\dot{H}$ is the deformation rate. In the derivation

of this equation it was assumed that R_3 is almost as large as R_1 and this is the case for aggregates which have been compressed by less than 50% of their original height.

The contribution of surface tension to the total force can be calculated using the radii of curvature and the aggregate medium surface tension and is simply a rearranged version of the Laplace equation described earlier.

$$F_{CM} = \pi\gamma_{CM} R_3^{\,2}(1/R_1 + 1/R_2) \qquad [5]$$
$$N \sim \frac{N}{m} \bullet m^2(\frac{1}{m} + \frac{1}{m})$$

The contribution of cell-cell interfacial tension can be determined via the following equation (Brodland, unpublished)

$$F_{CC} = \pi R_3^{\,2}(\sigma^{\gamma}{}_r - \sigma^{\gamma}{}_z) \qquad [6]$$
$$N \sim m^2(\frac{N}{m^2} - \frac{N}{m^2})$$

where $(\sigma^{\gamma}{}_r - \sigma^{\gamma}{}_z)$ is the difference between the radial and axial stress and relates to interfacial tension via the following equations (Brodland, unpublished):

$$\sigma_r^{\gamma} = \gamma_{cc} f_r^{\gamma}$$
$$\sigma_z^{\gamma} = \gamma_{cc} f_z^{\gamma} \qquad [7]$$
$$\frac{N}{m^2} \sim \frac{N}{m} \bullet \frac{1}{m}$$

2.5.3 Predictions of the DITH

Based on computer simulations based on DITH predict several behaviors of cells in media and cells in contact with other types of cells. For two types of cells 'A' and 'B' in media it is predicted that total engulfment will occur if the following criteria is met.

$$\gamma^{AB} \mathrel{f} \gamma^{AM} \qquad \text{and} \qquad \gamma^{AD} \mathrel{p} \gamma^{AM} - \gamma^{BM}$$

Where γ^{AB} is the tension between cells of type A and type B, γ^{AM} is the tension between cells of type A and the media and , γ^{BM} is the tension between cells of type B and the media.

For cells of type A and B to separate the following condition must be present: $\gamma^{AB} \mathrel{f} \gamma^{AM} + \gamma^{BM}$. That is the tension between cells of type A and cells of type B must be greater than the sum of the tensions between type A cells and the media and type B cells and the media. For cells of any given type dissociation will occur if the interfacial tension between the cells (γ^{AA}) is greater than the tension between the cells and the media (γ^{AM}).

In addition the DITH makes predictions for cells of two types in contact with each other. For two types of cells 'C' and 'D' with interfacial tension between them γ^{CD} and with interfacial tensions with cells of their same type γ^{CC} and γ^{DD} predictions can be made as to whether they will sort, mix, or form a checkerboard formation.

For sorting to occur the following criteria must be met $\gamma^{CD} \mathrel{f} \frac{\gamma^{CC} + \gamma^{DD}}{2}$. That is that the tension between cells of type C and D must be greater than twice that of the sum of the tension between two type C cells and two type D cells. For mixing to occur either $\gamma^{CD} \mathrel{p} \frac{\gamma^{CC}}{2}$ or $\gamma^{CD} \mathrel{p} \frac{\gamma^{DD}}{2}$ must be met. That is, that tension between cells of type C and D must be less than half of the tension of the tension between cells of the same type.

For a checkerboard formation to occur the tension between cells of type C and cells of type D must be approximately equal to $1/\sqrt{2} * \gamma^{CC}$ or be approximately equal to $1/\sqrt{2} * \gamma^{DD}$.

2.6 Cell Aggregate Formation, Staining, and Microscopy

2.6.1 Cell Aggregate Formation

Dissociated cells from chick embryonic tissue will reaggregate given the proper conditions. Components of the cell culture media, carbon dioxide, and gyration of the cell suspension are all involved in the cell aggregation process. Cells must be kept at a pH between 7.2 and 7.4 and in order to this a combination of a bicarbonate buffer with gaseous carbon dioxide and the chemical buffering agent HEPES (50). Bicarbonate is used with a carbon dioxide incubator kept at 5 % carbon dioxide. Gaseous carbon dioxide balances with HCO3/CO3 in the media to maintain the pH of the solution. HEPES (4-(2-hydroxyethyl)-1-piperazineethanesulfonic acid) carries both a positive and negative charge on different atoms within it which make it useful for buffering solutions (50). For aggregate experiments where compression is done outside of the controlled carbon dioxide environment a combination of HEPES and bicarbonate buffering is used (50). Antibiotics are used to prevent the growth of fungus and bacteria, which multiply faster than avian cells and will overtake the cell culture. DNAse is used to degrade free DNA which will increase the viscosity of the cell suspension solution and alter aggregation. Serum is a complex mix of albumins and growth factors. The type of serum used is important to cell aggregation studies; horse serum in culture media allows cells to aggregate, while fetal bovine serum does not result in cell aggregates under the same conditions (50). In addition to cell culture media, and the carbon dioxide conditions cells also require shaking on a gyratory shaker at speeds between 80 and 120 rpm.

2.6.2 Cell Aggregate Staining

Several dyes have the potential to allow for the visualization of cell shape, and these labels fall into the category of those dyes which are taken up by the cell and dye its contents and those which dye the membrane of the cell. In addition the dye must be

retained as the cells aggregate over a period of days. Cell Tracker Green (Invitrogen ®) is a chloromethyl derivative that freely diffuses through the membrane of cells. Once inside the cell the probe reacts with intracellular components to produce cells that fluoresce for at least twenty four hours (51). The mechanism by which it works involves esterase hydrolysis, which converts nonfluorescent CMFDA to fluorescent 5-chloromethylfluorescein, which can then react with thiols on proteins and peptides to form aldehyde-fixable conjugates. This probe may also react with intracellular thiol-containing biomolecules first, but the conjugate is nonfluorescent until its acetates are removed.It has a low pKa, which ensures it will fluoresce in the cytoplasm at physiological pH levels. Cells dyed with Cell Tracker Green can be used to form aggregates with undyed cells, allowing the cell shapes of dyed cells to be seen. DiO (Invitrogen ®) is a lipophilic carbocyanine which is weakly fluorescent in water but highly fluorescent and photostable when incorporated into membranes. Once applied to cells, it diffuses laterally within the plasma membrane, resulting in staining of the entire cell membrane. Transfer of these probes between intact membranes is usually negligible and DiO is well retained in cell membranes for long-term studies. When using a membrane dye the entire population of cells can be dyed or a mixed population can be used (51). PKH2 Green Fluorescent Membrane Label (Sigma-Aldrich) is a molecule made up of fluorescent dye moieties attached to long, lipophilic tails. During the membrane staining the lipophilic tails diffuse into the cell membrane, leaving the fluorescent moiety exposed near the outer surface of the cell. PKH2 is used to achieve stable, uniform staining for up to one hundred days and shows little transfer between cells (52).

2.6.3 Stained Aggregate Microscopy

With an aggregate containing stained cells, a confocal microscope can be used to observe cell shapes within the aggregate. The present study uses a spinning disc confocal microscope which consists of a thin wafer with hundreds of pinholes that are arranged in a spiral pattern. When a portion of the disc is placed in the internal light path of the confocal microscope, the spinning disc produces a scanning pattern of the subject. As the subject is inspected, light is reflected back through the microscope objective. The light

that was reflected from in front of or behind the focal plane of the objective approaches the disc at an angle rather than perpendicularly. The pinholes of the disc permit only perpendicular rays of light to penetrate. This enables the microscope to view a very thin optical section of tissue. In addition pictures can be captured at a high rate since the scanning speed of the laser used in other confocal systems is not a factor.

Chapter 3 Measurement of Surface Tension

3.1 Introduction

In this chapter the measurement of surface tensions for aggregates of chick embryonic cells is detailed. Aggregate surface tension refers to the tension between the aggregate and its surrounding media. Surface tension measurements give meaningful information about how cells are likely to interact and can predict sorting and engulfment behaviors between two populations of cells (10). Surface tension measurements have been made in various types of tissues including embryonic chick tissues (2, 4), various types of tumors (6-8), and pancreatic islet cells (5). Aggregated embryonic chick cells were compressed and the force required for compression as well as the radii of curvature were measured in order to determine surface tensions. Confirmation of aggregate liquidity was accomplished through comparison of surface tension values from two successive compressions and by comparing surface tensions over a range of aggregate volumes. In addition the compression system was further validated via the measurement of the surface tension of water.

3.2 Experimental Procedures

3.2.1 Preparation of Cell Aggregates

Fertile White Leghorn chicken eggs (Shaver Poultry Breeding Farms Ltd. Ontario, Canada), were incubated at 37°C and 50% humidity for 5 days. Neural retina, heart, mesencephalon and livers were obtained from 5-day embryos. Dissections and dissociations were adapted from previously published methods (2). Briefly, dissociations of dissected tissue fragments were conducted in calcium and magnesium-free Hanks'

Balanced Salt Solution (HyQ ®). Tissues were dissected and placed into a solution of ice cold 0.25% trypsin (Gibco ®). Dissected tissues were kept at 4 °C for 3 hours. Excess trypsin was removed and tissues were incubated in residual trypsin at 37°C until tissue came apart with gentle pipetting. To stop trypsin action 1 mL of a solution containing 50 % Horse Serum (Gibco ®), 50% complete media was added. Complete media consisted of MEM/EBSS (HyQ®) with 50 mg/ml DNase I (Roche Diagnostics), 26mM bicarbonate, 10 mM HEPES, 10% horse serum and the following antibiotics: 70 mg/ml genetamycin (Gibco ®), 50 mg/ml penicillin/streptomycin/neomycin (Gibco ®) and 50 mg/ml kanamycin (Gibco ®). After addition cell solutions were centrifuged at 2000 RPM for 4 minutes to settle the cells. Supernatant solution was removed and cells were resuspended in 1 mL complete media. Cell concentrations were estimated using a haemocytometer, and cell viability was determined using trypan blue. Cells were diluted to 3 x 10^6 cells/ml and 3 ml was transferred to 5 ml round bottom flasks. Flasks were placed in a water bath/shaker at 37°C, 5% CO_2 for 1-2 days at 120 rpm for one to three days prior to aggregate compression tests.

3.2.2 Aggregate Compression

The apparatus used to measure the surface tension of the embryonic aggregates consisted of an aluminum plate for the aggregates to rest on and an upper Zaber-controlled beam used to compress the aggregates. Multidiameter aggregates of chicken embryonic cells ranging in diameter from 100 to 500 μm were compressed between the beam and the bottom plate in CO_2 indpedent media (Sigma®) heated to 37 °C. A force transducer was used to measure the force required to compress the aggregate over time. The plate and the beam were coated with poly(2-hydroxyethylmethacrylate) to minimize the adherence of the aggregate to the apparatus. The upper beam is Zaber-controlled and positioned using a game controller and the compression is controlled via Tissue GUI software and images are captured continuously at a rate of about 1 per second as compression occurs.

3.2.3 Radii of Curvature and Surface Tension Calculation

Zazu software was used to analyze the image and obtain the radii of curvature and these values are subsequently used with the force value to calculate surface tension. To determine the radii the user must manually outline the aggregate, and input the pixels per millimeter in the image. With this information the radii of curvature are calculated in micrometers. The user also manually inputs the point where the aggregate and plate no longer contact each other. Figure 3.1 shows a screenshot of an aggregate, the outline of an aggregate and the radii of curvature. The image has 1355 pixels per millimeter and the radii of curvature values are shown.

These radii are used in equation 5 to determine the surface tension.

$$F_{CM} = \pi \gamma_{CM} R_3^2 (1/R_1 + 1/R_2) \qquad [5]$$

3.2.4 Calculation of Surface Tension of Water

The compression apparatus was used to compress air bubbles placed between the beam and the plate for calibration purposes. Compression took place in the same manner as for the compression of aggregates with the exception that several of the tests took place in distilled water.

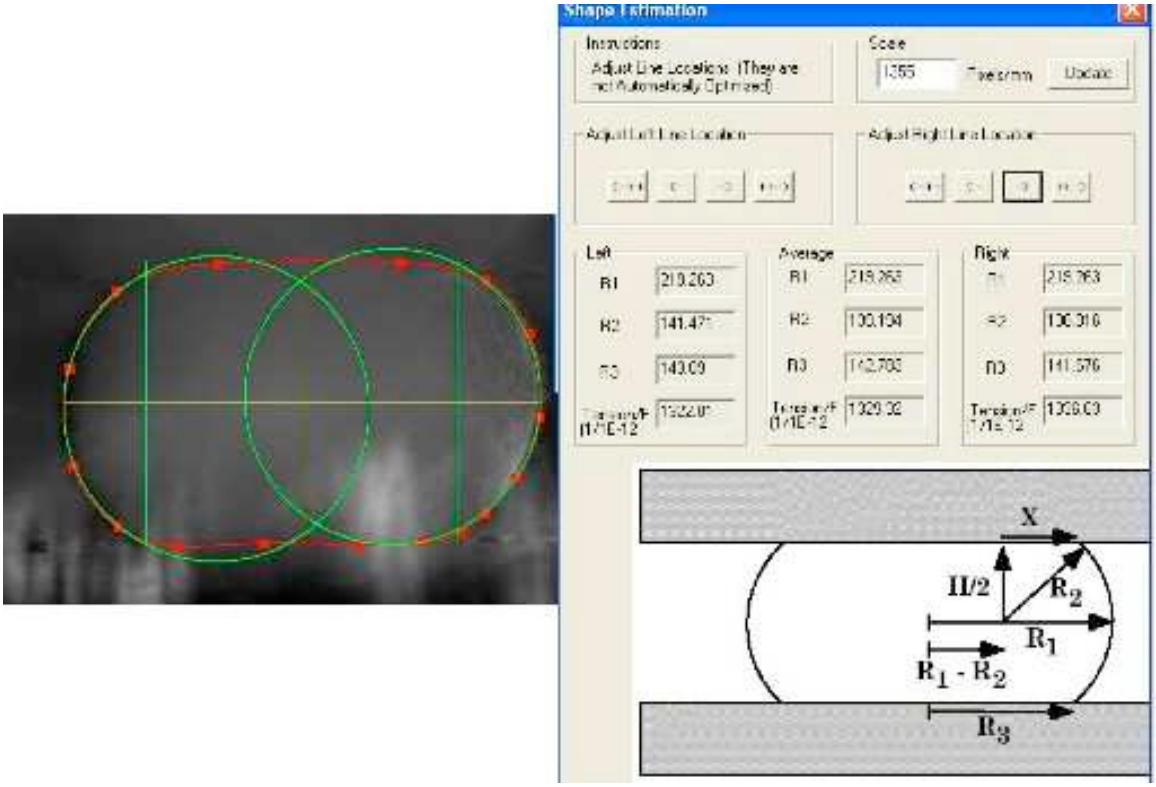

Figure 3.1 Screenshot of aggregate outline and radii of curvature. User manually outlines aggregate boundaries and adjusts the right and left line locations (left). Zazu software outputs radii of curvature (right).

3.3 Results and Discussion

3.3.1 Measurement of Chick Embryonic Aggregate Surface Tension

Force time curves and aggregate profiles were obtained for several tissues in order to determine the surface tension of each tissue. Aggregates of chick heart, liver, mesencephalon, and neural retina embryonic tissue were compressed and surface tensions were measured. A typical force-time curve from an aggregate of heart cells is shown in Figure 3.2. The maximum force required to compress the aggregate decayed rapidly in the first five seconds and then slowly approached equilibrium. The initial rapid decay is thought to be from the elastic properties of the aggregate (3) and corresponds to the force required to deform the cytoplasm (14). Once the aggregate is at equilibrium the force acting to compress the aggregate is from the surface tension alone and can be used to calculate surface tension.

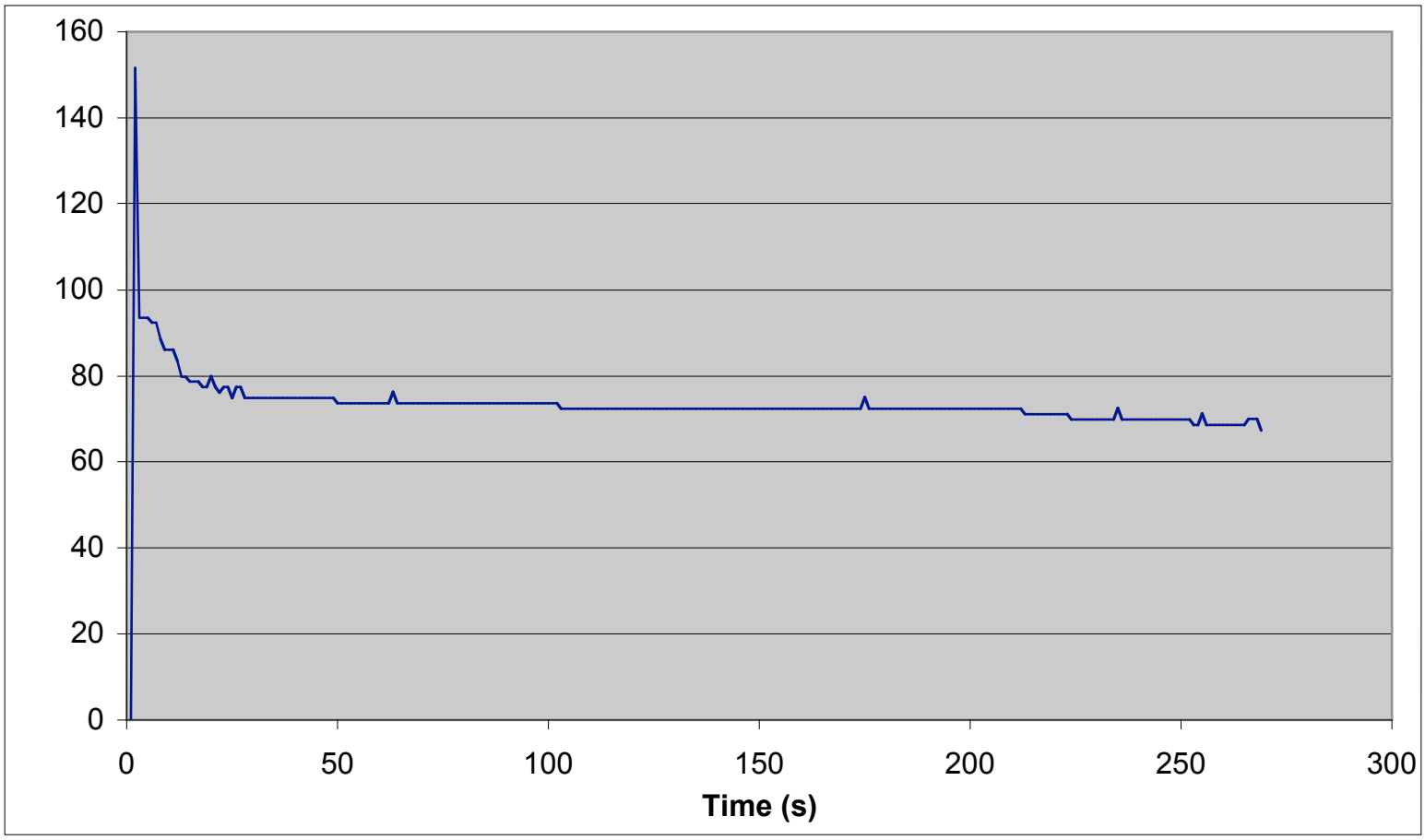

Figure 3.2: Force-Time curve for the compression of an aggregate of embryonic heart cells. The force increased rapidly as the area between the aggregate and the plate increased. Once compression stops the force continues to decay until it reaches an equilibrium state. The force required to compress the plate at this point is used to calculate the surface tension. Force is shown in micronewtons, time is shown in seconds.

In addition to the force required to compress the aggregate in its equilibrium state the radii of curvature were determined. As the aggregate was being compressed images of the aggregates profile were captured approximately every second. The final image captured during compression was analyzed using Zazu software in order to determine these radii.

With the radii of curvature and force required for compression at equilibrium, surface tension values were determined using equation 5. Surface tension values along with radii of curvature and measured forces at equilibrium are shown in Table 3.1.

Table 3.1 Surface Tension Values for Aggregates of Embryonic Chick Tissue

Tissue	Trial	R_1 (μm)	R_2 (μm)	R_3 (μm)	F (μN)	γ_{CM} (mN/m)
Neural Retina	1	218.9	60.3	162.9	30.51	1.7
	*2	192.9	141.7	139.5	21.85	2.9
	3	227.1	63.7	180.0	28.23	1.4
	4	265.4	56.0	207.2	37.52	1.3
	*5	255.6	65.3	190.0	13.02	0.6
Liver	1	301.7	90.1	248.1	56.52	2.0
	2	171.1	63.7	119.8	16.19	1.7
	3	123.9	85.9	86.7	8.68	1.9
	3b	154.8	51.5	110.2	19.60	2.0
	4	132.7	59.9	98.8	20.51	2.7
	*5	285.4	133.6	203.4	16.07	1.2
Heart	*1	241.6	119.4	168.0	39.92	3.5
	1b	259.2	99.6	181.4	67.94	4.7
	2	211.9	122.3	148.4	51.70	9.3
	2b	163.2	82.1	105.0	61.13	8.4
	3	219.3	139.2	142.8	51.70	7.2
	3b	229.3	148.4	187.5	136.80	11.1
Mesencephalon	1	219.4	94.9	160.9	16.55	1.4
	2	220.2	89.9	151.1	11.55	1.1
	1d	383.1	94.6	268.2	43.11	1.4
	2d	386.5	94.8	228.1	27.47	1.4

Notes: * indicates test with aberrant force-time curve, b indicates second compression on same aggregate, d indicates aggregates which were dyed with PKH2.

For mesencephelon tissue some aggregates were dyed with PKH2 Green Fluorescent Membrane label (Sigma-Aldrich) to visualize cell shapes, these results are

marked with a ‘d’ and are further discussed in Chapter 4. Also tests marked ‘b’ indicate that this was the second compression on the same aggregate. The results of these tests are discussed in section 3.3.2.

Certain tests which are marked with an asterisk (*) showed a sudden unusual increase or decrease in force after it appeared an equilibrium state had been reached. For these tests the apparent equilibrium value was used for adjusted surface tension measurements. The unusual changes may have been a result of the aggregate adhering to the beam or the base plate. Although contact surfaces were coated in poly(hema) to reduce adherence, some adherence to the apparatus may have occurred and has been noted in compression studies done by other groups (4). For *-marked tests the force value at equilibrium and before the unusual change was used to recalculate the surface tension. The adjusted results are shown in Table 3.2. Values were taken at the following time points for Neural Retina Trials 2 and 5 forces were determined at 90 and 120 seconds respectively, for Liver Trial 2 and Heart Trial 1 the force was determined after 90 seconds. Force time curves for all tests are shown in Appendix A.

Table 3.2 Adjusted Surface Tension Values for Chick Embryonic Tissue Aggregates

Tissue	Trial	R_1 (μm)	R_2 (μm)	R_3 (μm)	F (μN)	γ_{CM} (mN/m)
Neural Retina	1	218.9	60.3	162.9	30.51	1.7
	*2	192.9	141.7	139.5	14.03	1.9
	3	227.1	63.7	180.0	28.23	1.4
	4	265.4	56.0	207.2	37.52	1.3
	*5	255.6	65.3	190.0	13.02	0.8
Liver	1	301.7	90.1	248.1	56.52	2.0
	2	171.1	63.7	119.8	16.19	1.7
	3	123.9	85.9	86.7	8.68	1.9
	3b	154.8	51.5	110.2	19.60	2.0
	4	132.7	59.9	98.8	20.51	2.7
	*5	285.4	133.6	203.4	36.16	2.8
Heart	1	241.6	119.4	168.0	56.04	5.0
	1b	259.2	99.6	181.4	67.94	4.7
	2	211.9	122.3	148.4	51.70	9.3
	2b	163.2	82.1	105.0	61.13	8.4
	3	219.3	139.2	142.8	51.70	7.2
	3b	229.3	148.4	187.5	136.80	11.1
Mesencephalon	1	219.4	94.9	160.9	16.55	1.4
	2	220.2	89.9	151.1	11.55	1.1
	1d	383.1	94.6	268.2	43.11	1.4
	2d	386.5	94.8	228.1	27.47	1.4

Notes: * indicates test with aberrant force-time curve, b indicates second compression on same aggregate, d indicates aggregates which were dyed with PKH2.

Similar compression tests have been performed and surface tension values reported. Table 3.3 shows values from previous similar studies in addition to values determined in this study. Averages and standard deviations are shown in mN/m.

Table 3.3 Aggregate Surface Tension Values From Several Studies

Tissue	Non Adjusted (mN/m)	Adjusted (mN/m)	Foty (1994) (mN/m)	Foty (1996) (mN/m)
Heart	7.4 ± 2.8	7.5 ± 2.5	8.3 ± 0.1	8.5 ± 0.2
Liver	1.9 ± 0.5	2.2 ± 0.5	4.3 ± 0.1	4.6 ± 0.1
Neural Retina	1.6 ± 0.9	1.4 ± 0.4	/	1.6 ± 0.1
Mesencephalon	1.3 ± 0.2	/	/	/

Our measured values were in close accordance with those measured by Foty et al, 1994. Differences between the two sets of values could be a result of the differences in the apparatus as our force transducer setup and analysis were different from those used in studies by Foty et al shown above. Initially we used a thicker shorter beam, which did not give high enough force resolution to resolve the small forces involved in surface tension measurements. The thinner, longer beam allowed for increased force resolution results but for some tests there was still a significant amount of rapid changes that occurred in the force measurements between single second time points. It is unlikely that the force required to compress the aggregate would increase and decrease as rapidly as was shown therefore it may be that further alterations to the force transducer are necessary and that varying widths and lengths of beams need to be tested. A beam that did not give precise force measurements would also account for the higher standard deviation shown in our results.

3.3.2 Confirmation of Liquid-Like Behavior

For a tissue to be considered liquid the measured surface tension values should be constant over a range of aggregate sizes as well as applied forces. For several aggregates a second force was applied to the same aggregate to verify their liquid-like properties. Surface tension values where two compressions were performed are shown in Table 3.4. Values are shown in mN/m.

Table 3.4 Comparison of Two Successive Compressions

	1st compression (mN/m)	**2nd compression (mN/m)**
Liver Trial 3	1.9	2.0
Heart Trial 1	5.0	4.7
Heart Trial 2	9.3	8.4
Heart Trial 3	7.2	11.1

These tests showed similar surface tension values when the aggregate was subjected to a second greater compression. For Heart Trial 3 the second compression yielded a substantially higher surface tension value indicating that the aggregate may have lost or begun to lose its liquid like properties. If the first compression was too great the

aggregate may not have recovered and may not have responded in a liquid-like way to the second compression.

In addition to obtaining similar surface tension values when different forces are applied, surface tension should be independent of volume for an aggregate to be considered liquid. Aggregate surface tension did not show a correlation between surface tension and volume of the aggregate. Surface tension values are plotted against aggregate volumes for various tissues in Figure 3.3. This analysis was done for a wider range of aggregate sizes in Foty's experiments (3) and aggregates of liver were shown to have fairly constant surface tensions within a 9-fold range of volumes. Our tests had a smaller range of test volumes but also showed a lack of correlation between volume of aggregate and surface tension indicating that the aggregates were acting as liquids.

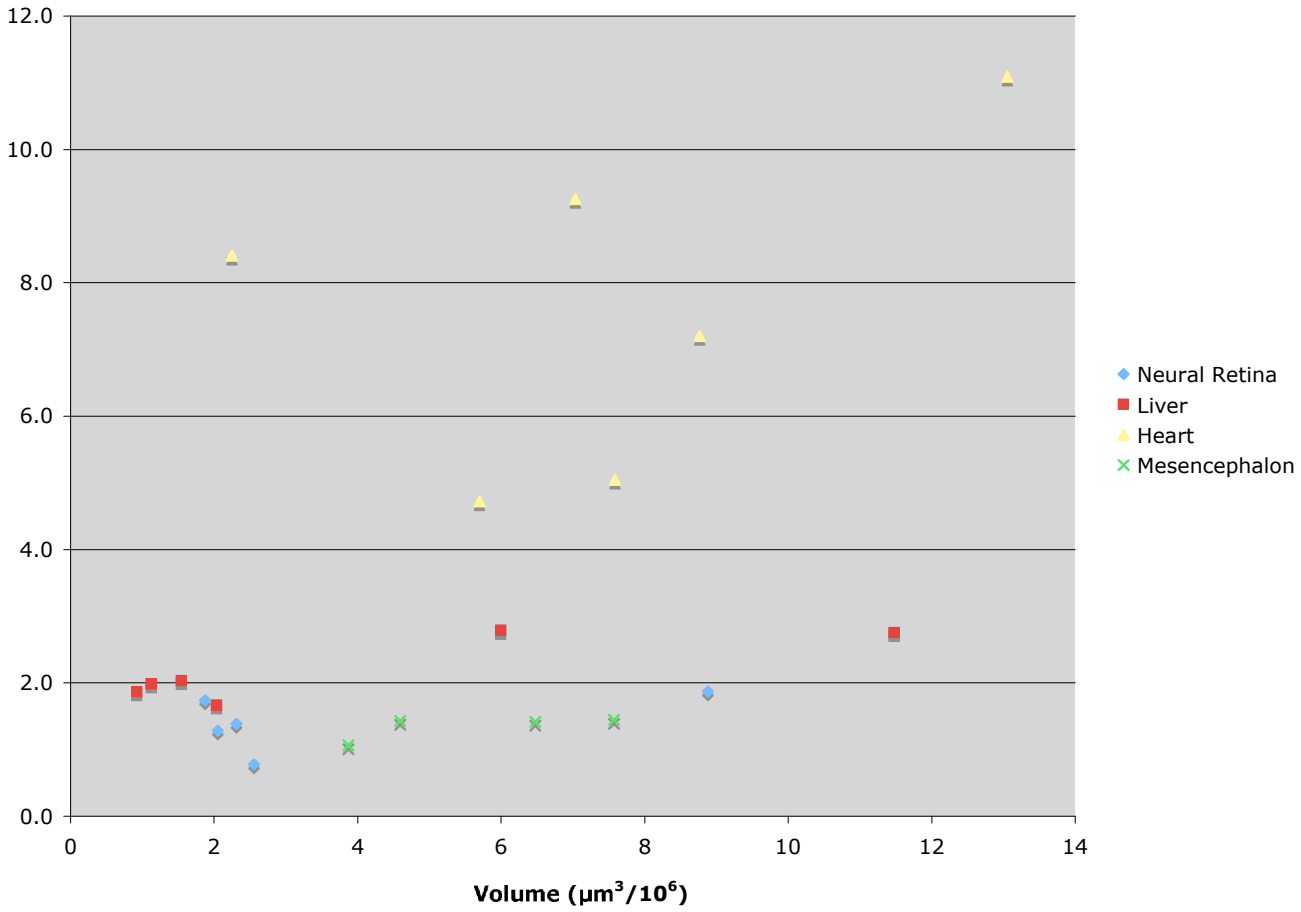

Figure 3.3 Correlation between volume of aggregate and surface tension. Surface tension values do not change based on aggregate size. Neural Retina and Liver aggregates show similar surface tensions across a 5-fold range of aggregate volumes.

3.3.3 Measurement of Surface Tension of Water

In order to further test the accuracy of the surface tension measurements made using the compression device the surface tension of water was measured by compressing an air bubble in the device. Results of bubble compression tests are shown in Table 3.5.

Table 3.5: Measurement of the Surface Tension of Water

	Force (μN)	Surface Tension (mN/m)
water-air	71.91	40.8
water-air	171.35	63.6
water-air	369.74	139.8
water-air	340.30	80.7

The accepted value for the surface tension of water is 72.8 mN/m at room temperature. Using our compression device we obtained an average surface tension value of 81.2 mN/m with a standard deviation of 42.3 mN/m. The average value is consistent with the accepted value. However; the standard deviation is quite high. The sizes of the air bubbles were very large in comparison the cell aggregates some being larger by a factor of close to 10. An explanation for the high standard deviation could be that the apparatus does not consistently measure surface tension for larger volume bubbles with greater forces required for compression. The forces being measured at equilibrium for the aggregates were in the range of 10 μN to 100 μN while for the water tests the forces ranged from 70 μN to 300 μN. The measurement of the surface tension of water may have been more precise if smaller bubbles that required less force to compress were used for tests.

3.3.4 Concluding Remarks

Overall the results indicate that we were successful in the measurement of surface tension values of both embryonic chick tissue and water. Values were consistent published results as well as accepted values. The tests showed that the aggregates displayed liquid-like surface tensions as the values of surface tension were independent of aggregate size and compression force. In addition, according to DAH, surface tension measurements can predict the mutual envelope behaviors of tissues. It was found that

heart is enveloped by liver, which is enveloped by neural retina (3). Our surface tension results would predict the same envelope behavior demonstrated in their experiments.

The standard deviation was high for the measurement of surface tension of water as well as for the measurement of embryonic surface tensions. This indicates there may be high amount of variability associated with the apparatus. This could be a result of the beam thickness in the force transducer and that it may require adjustment for varying sizes of aggregates to obtain more precise force measurements.

Chapter 4 Measurement of Interfacial Tension

4.1 Introduction

Interfacial tension refers to the cumulative force that acts along the edges of cells. It includes forces derived from cell adhesions, cytoplasmic viscosity, and microfilaments (14) and is referred to as cortical tension in some literature (1). Recent research has indicated that adhesion alone does not account for sorting behavior and that actin dynamics are likely to play a role (1). Computer simulations have shown that the value of interfacial tension can be determined if in addition to the force time compression curve and the radii of curvature, the geometry of cells within the aggregate being compressed are monitored. In this section the steps required to measure interfacial tension are detailed.

4.1.1 Visualizing Cell Shapes Within an Aggregate

In order to monitor cell shapes as an aggregate is being compressed, several setups of the microscope and compression device can be used. A compression device to be used with an inverted microscope would compress the aggregate horizontally as shown in Figure 4.1 A, where as a microscope that viewed the aggregate profile could use a compression device that compressed the aggregate vertically as shown in figure 4.1 B.

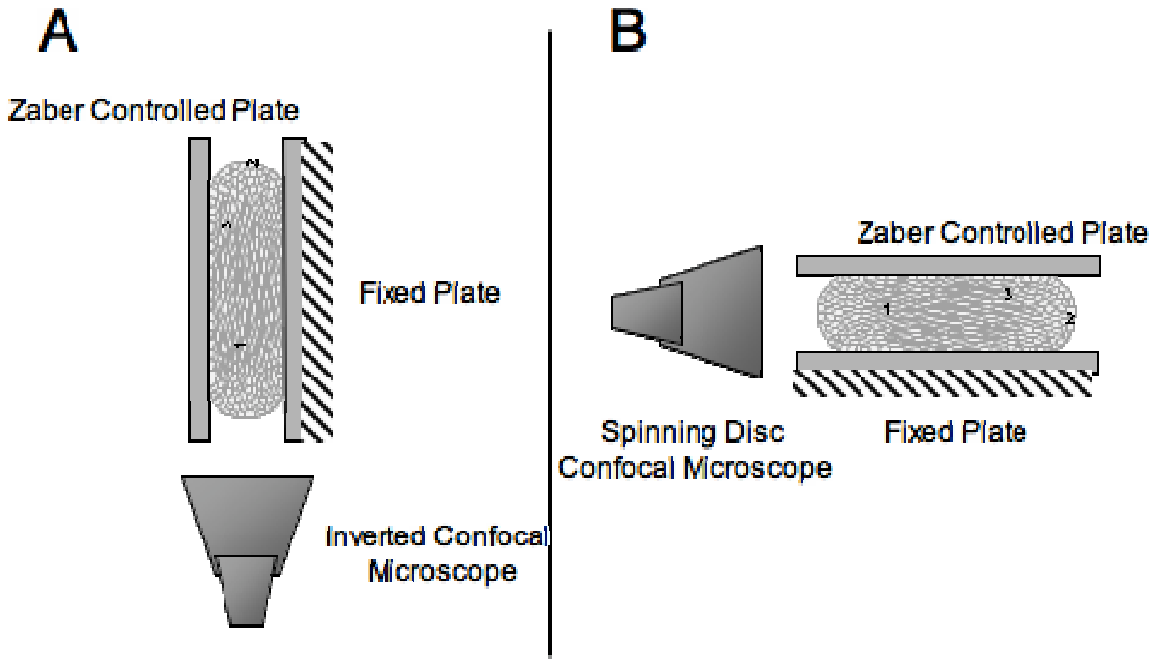

Figure 4.1: Schematic of horizontal and vertical compression setups for viewing cell shapes. (A) shows the horizontal compression device developed for use with an inverted confocal microscope. (B) shows the verticle compression device developed for use with the spinning disc confocal micrscope.

4.1.2 Fluorescent Labeling of Cells

Dyes which are retained in cell culture over a period of days were used to visualize cells within the aggregate during compression tests. Several fluorescent labels were tested and they either stained the entire cell or stained the membrane of the cells. In these experiments Cell Tracker Green (Invitrogen ®), DiO (Invitrogen ®), and PKH2 (Sigma-Aldrich) were analyzed for use in visualizing cell shapes during aggregate compression tests.

4.2 Experimental Procedures

4.2.1 Dyed Aggregate Preparation

Aggregates were prepared in the same manner as described for surface tension measurements except that, dye, either cell tracker green, DiO or PKH2 was added to the cell suspension after trypsin action was stopped. DiO was applied according to product instructions for cells in suspension and cells were incubated for 20 minutes in a 25 uM solution of DiO in serum-free MEM. Cell Tracker Green was applied according to product instructions and cells were incubated for 30 minutes in a 10 uM solution. PKH2 Green Fluorescence Linker Kit was used according to product instructions and cell suspension was incubated in a 2 uM solution of PKH2 in Diluent A (Sigma-Aldrich) for 3 minutes. For cell dyes which stained the entire cell a mixed suspension consisting of 70% stained and 30% unstained cells were allowed to aggregate.

4.2.2 Compression Device Development

Several compression setups were attempted in order to visualize cell shapes while an aggregate was being compressed. A horizontal compression device was developed for use with an inverted confocal microscope. An aggregate was placed between two plates one of which was fixed. A Zaber-controlled plate was used to compress the aggregate against the fixed plate and an inverted confocal microscope was used to monitor cells during compression.

4.2.3 Force-Time and Cell Shape Data Collection

During aggregate compression images were captured at approximately 1 image per second. Labeled cells were observed during compression as well as the profile of the aggregate. Force-Time curves were obtained in the same manner as for the measurement of surface tension in Chapter 3.

4.3 Results and Discussion

4.3.1 Comparison of Vertical and Horizontal Compressions

Two types of compression devices were used in attempts to measure interfacial tension. The first attempt involved horizontal compression of the aggregate while the aggregate profile and cell shapes were monitored from the bottom, the second device monitored cell shapes from the side during a vertical compression.

The first horizontal compression device is diagrammed in figure 4.1 A. Several aggregates were compressed with this device although no force measurements were taken as aggregates were prone to slipping under the Zaber-controlled plate upon compression. Cell shapes were visible using DiO with this apparatus but because compression could not be done so it is not known whether changes in shape could be monitored during compression. Images captured before compression are shown in Figure 4.2.

The second device that was developed is diagramed in Figure 4.1 B. With this device aggregates could be compressed vertically eliminating the problem of aggregates slipping under the plate during compression. Using this device surface tension values were measured and dyed cells could be seen during compression. Several trials of compression tests were done where cell shapes could be seen. However changes in cell shape were not apparent. In addition in order to calculate surface tension both the aggregate profile and the shapes of the cells within the aggregate must be observed simultaneously. In order for cell shapes to be clear the 20x objective was used. However, at this magnification the field of view was smaller and the aggregate profile could not be seen for larger aggregates.

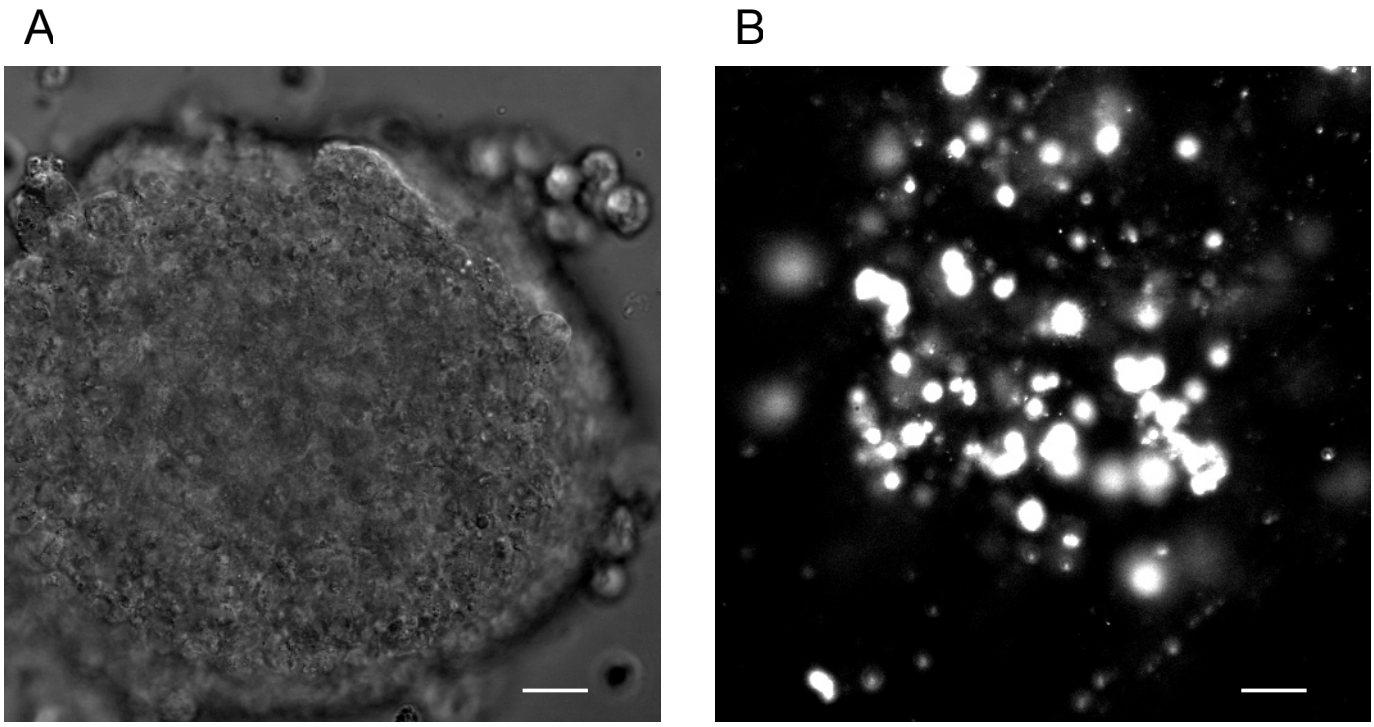

Figure 4.2: Confocal images of cell aggregate showing cell shapes. A shows a D-channel image of an aggregate stained with DiO, B displays the same aggregate with DiO labeled cells fluorescing. Cell aggregate is approximately 300 μm in diameter, scale represents 25 μm.

Overall the vertical compression device showed more promise than the horizontal device. In addition images could be captured faster using the spinning disc confocal microscope compared to the inverted microscope.

4.3.2 Effect of Dye on Surface Tension Values

Aggregates made from cells stained with PKH2 green fluorescent membrane label (Sigma-Aldrich) were prepared concurrently with unstained aggregates. Surface tension values were compared in order to determine if staining the cells affected the surface tension values. Two trials were performed with dyed mesencephalon aggregates and two trials without dye. Results are shown in Table 4.1.

Table 4.1 Surface Tension Values for Dyed Aggregates and Undyed Aggregates

Tissue	Trial	R_1 (μm)	R_2 (μm)	R_3 (μm)	F (μN)	γ_{CM} (mN/m)
Mesencephalon	1	219.4	94.9	160.9	16.55	1.43
	2	220.2	89.9	151.1	11.55	1.07
	1d	383.1	94.6	268.2	43.11	1.45
	2d	386.5	94.8	228.1	27.47	1.41

These results show that dying the cells with PKH2 did not have an effect on the surface tension of the aggregates. In addition sorting experiments with N-cad-transfected L cells involved the use of PKH2 as a cellular marker to distinguish one type of cell line from another (49).

4.3.3 Analysis of Images Using Various Cell Dyes

Several cellular and membrane dyes showed promise for use with chick embryonic aggregates. PKH2 was used by Foty et al (10) in sorting experiments, DiO is used for long term tracking experiments and was retained in cells for long periods of time as was cell tracker green. In order to obtain confocal images where cells shapes are visible the dye had to fluoresce with sufficient intensity. Several trials with each dye were performed and representative aggregates stained with each dye are shown in Figure 4.3. DiO showed strong fluorescence but outlines of cells could not be seen, while Cell Tracker Green did not show strong enough fluorescence to capture confocal images. PKH2 fluoresced very strongly and the outline of cells could be seen.

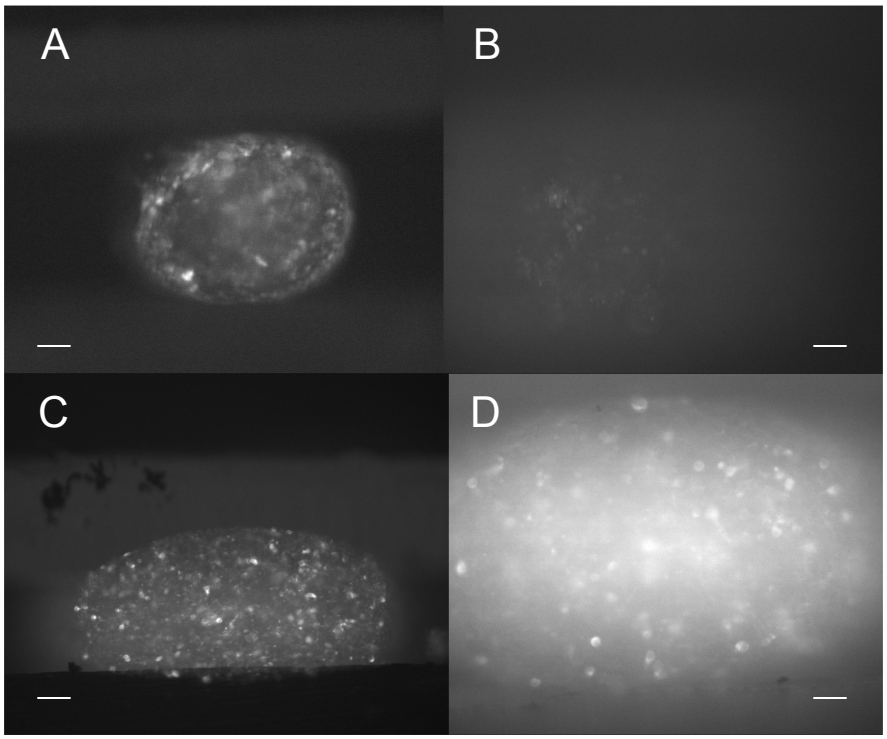

Figure 4.3 Confocal optical sections of embryonic chick cell aggregates captured during compression with different cell stains. A and B show aggregates of heart cells from a 5-day-old chick embryos. In A cells were dyed with DiO, while in B cells were dyed with Cell Tracker Green. C and D show aggregates of Mesensephalon cells from 6-day-old chick embryos dyed with PKH2. A-C show images taken with the 10 x objective and D shows an image taken with the 20 x objective. Scalebar shows 60 μm in A-C and 30 μm in D.

4.3.4 Analysis of Compressions

Several compressions of aggregates stained with PKH2 were performed. Initially the microscope was focused on individual cells inside the aggregate prior to compression, however once compression took place these cells would be out of focus. In order to account for the movement of the aggregate during compression the software was rewritten so that the stage would move a number of microns inputted by the user. The distance varied from 3 micrometers to 12 micrometers and was a trial and error process. The distance depended on the size of the aggregate and degree of compression but several 10 second trial compressions were often necessary to find the ideal distance to focus on one layer of cells.

This adjustment worked well but images were not being captured rapidly during the initial compression, which is the time during which cells round up. Several rounds of compressions were done in this way but changes in cell shapes were not captured. A set of images from a representative compression is shown in Figure 4.4. The first 4 images captured are shown at 1, 7, 8, and 10 seconds. At this point images could be captured at a rate of 1 image per second. Images from 11, 12, 50, and 112 seconds after compression are shown. Although cell shapes are visible in these images no changes could be seen during compression.

Subsequently the software was changed so that images could be captured more rapidly after the initial compression. Several compression tests were done using this setup, however changes in cell shape were still not apparent. A sample compression is shown in Figure 4.5. Images were captured at a rate of 1 image per second and the first 10 images are shown.

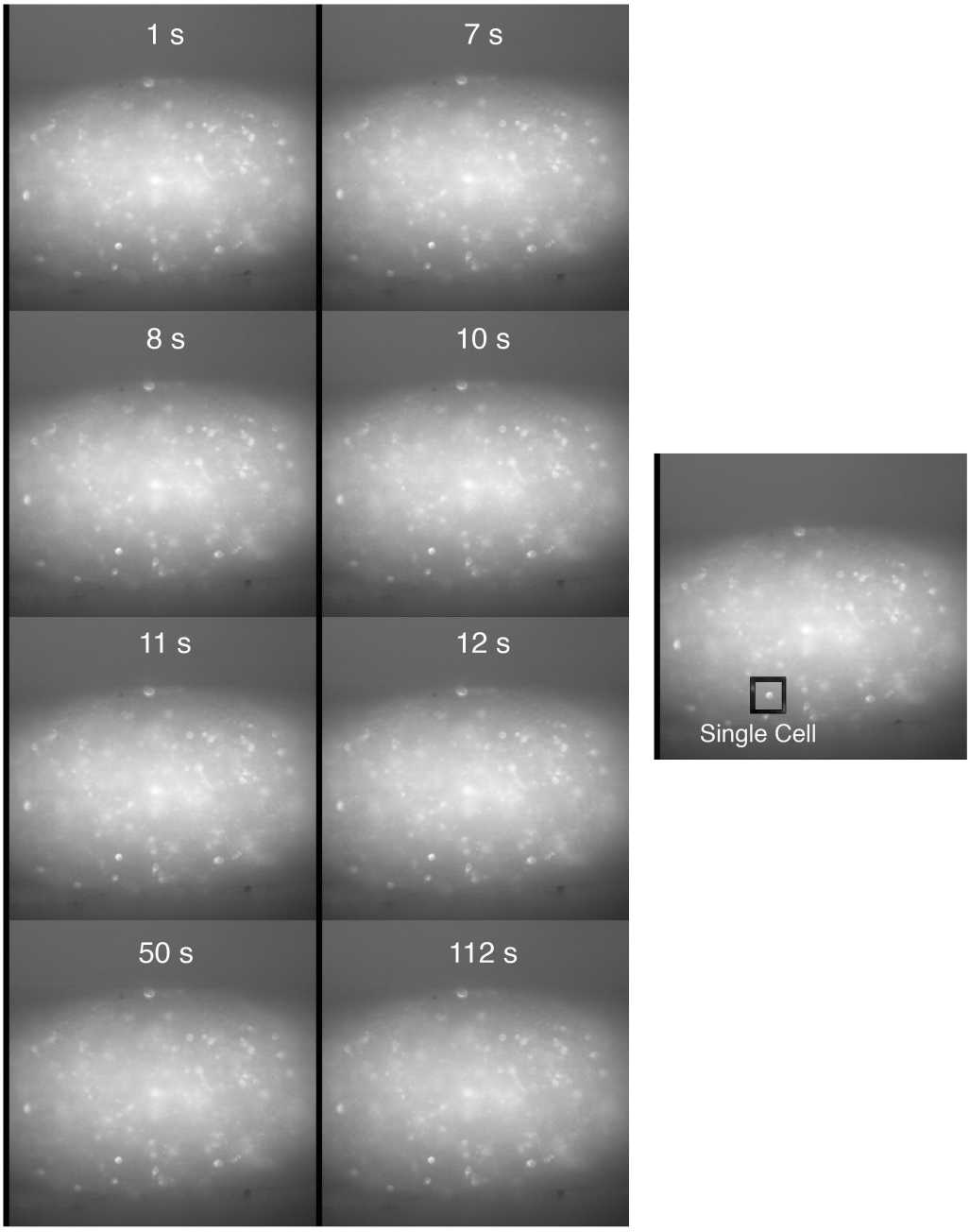

Figure 4.4: Confocal images of aggregate during compression. The first 4 images captured are shown at 1, 7, 8, and 10 seconds. At this point images could be captured at a rate of 1 image per second. Images from 11, 12, 50, and 112 seconds after compression are shown. Although cell shapes are visible in these images no changes could be seen during compression. A single cell within the aggregate is shown within the black box on the right.

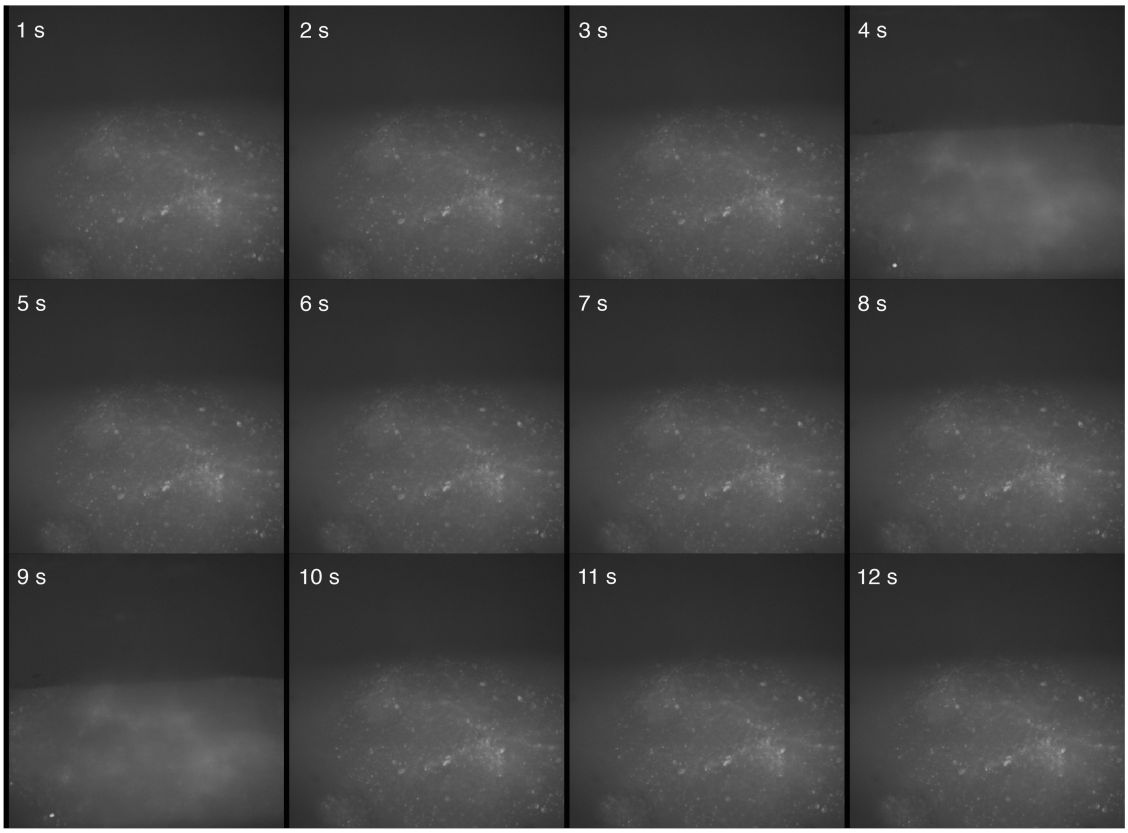

Figure 4.5 Confocal images of aggregate during initial 12 seconds of compression. A sample compression is shown in Figure 4.3.2. Images were captured at a rate of 1 image per second and the first 12 images are shown. In previous rounds of testing the images from the first 12 seconds were not captured. Scale bar shows 40 µm.

These images were analyzed using software designed to determine shapes of cells but due to image quality cell geometries could not be determined. Light from stained cells in front and behind the plain of focus appear to create a haze over the image which made image analysis more difficult.

There are several possible reasons we were unable to observe changes in cell shape associated with compression. One explanation is the resolution and quality of the images. It is possible with clearer images changes in cell geometry could be resolved. Our images were clouded by light from labeled cells out of the plane of focus. It is possible that this could be improved with a different type of dye, or a different cell type. Amphibian cells are larger and could be easier to resolve or another type of dye may require a shorter exposure time and less haze in the background of the image. In addition dying fewer cells within the aggregate could also eliminate the haziness from the background and allow for cell shapes to be resolved. Another explanation is that the cells are not changing shape over the course of our compression. Although simulations predict the cell shape changes would occur during the initial stage of compression results of compression through centrifugation showed cell shapes took much longer to occur (4). Finally, it could be that the changes in shape are occurring very rapidly at the beginning of compression and our images were not being captured at a rate that allowed the changes to be observed.

4.3.5 Concluding Remarks

Although we were unable to measure interfacial tensions of cells we were able to see cell shapes within an aggregate. Interfacial tensions if measured hold promise for providing information needed to link actin dynamics and cell adhesion and provide insight into cell interactions and behaviors and for this reason research into measuring these values should be continued. Alterations to the experimental method including a longer time course to the experiment or staining fewer cells within the aggregate as well as trying different types of cells or cell labeling could allow for interfacial tensions to be measured with the compression apparatus.

Chapter 5 Future Directions

5.1 Future Experiments Measuring Surface Tension

A range of biological phenomenom can be explained by the regulation of cell surface tension (1). For this reason the measurement of surface tensions can provide valuable information to many fields of biology.

5.1.1 Investigation of the Contribution of Actin Dynamics to Surface Tension

One area of debate in research on the surface properties of cells is whether cell sorting and surface tension values are a direct result of binding specificity between cadherin molecules or if other factors such as actin dynamics come into play. Experiments by Steinberg and Foty aimed to show that cell population behaviors including tissue segregation, mutual envelopment and sorting out are a direct result of surface tensions which are a direct result of adhesion forces from cadherins (10). Other research groups have made a case for the role of actin dynamics in surface tension and sorting behaviors (1, 12, 13, 47). Experiments done by Steinberg and Foty used cell lines with varied levels of cadherin expression and showed that there was a direct correlation between cadherin expression level and surface tension. Similar conclusions could be drawn about actin dynamics if altering actin polymerization resulted in altered surface tension values.

5.1.2 Investigation of Cancer Drugs on Surface Tension of Tumor Cell Lines

Surface tension measurements could also benefit cancer research. Surface tension values have been shown to predict the metastatic potential of cancer cells (6,7,8). Anti-cancer agents could be added to cell culture of aggregating tumour cell lines and it could be determined whether the treatment altered the surface tension of the aggregates.

Surface tension measurements have been used to determine whether or not tumour cells will invade surrounding tissue and whether treating tumour cells with various agents could inhibit their invasive capabilities. This could be done very simply without the use of model organisms often used to test tumor cell invasiveness.

5.2 Additional Steps Needed to Measure Interfacial Tension

Interfacial tensions may prove to be of great interest with regards to cell interactions. In order to measure these values changes in cell shape must be observed during compression. Experiments done by Forgacs (4) showed shape changes in cells compressed and fixed under centrifugation. After 5 minutes of centrifugation cells appeared elongated as did the aggregate but after 36 hours of centrifugation cells had rounded up. This indicates that perhaps our time course of 200 seconds may have been too short to see shape changes. However, computer simulations of DITH predict shape changes to take place during the rapid relaxing phase of compression that occurs in the first few minutes.

The centrifugation experiments may have different time course due to the difference in how the compression force is applied and the magnitude of force. The forces are not monitored during these experiments as they are in compression tests so it is unclear at what point during relaxation on a force-time curve the cells rounded up at. In order to determine if cell changes are taking place over a longer time course, compression of aggregates over a longer time period could be done and shapes of cells could be monitored for change. If changes are seen this would indicate that a longer time course is needed for our compression experiments and the initial time course prediction needs to be reevaluated.

5.3 Additional Experiments to Test DITH

Once interfacial tensions could be measured between cells of the same type, the surface tension could be compared to the interfacial tension in order to determine if the surface tension must be less than twice the interfacial tension in order for dissociation to occur as predicted by the DITH.

The other predictions described in section 2.5.3 require the interfacial tensions between two types of cells to be measured. To do this cell shapes of two different types

of cells must be determined while they are adjacent. This property would be more difficult to measure but may be done using multi-color labels of cells and compression of an aggregate containing the two cell types.

References

1. Lecuit, T. L.,Pierre-Francois 2007. Cell surface mechanics and the control of cell shape, tissue patterns and morphogenesis. Nat. Rev. Mol. Cell Biol. 8, 633-644.

2. Foty, R. A., G. Forgacs, C.M. Pfleger and M.S. Steinberg 1994. Liquid properties of embryonic tissues: Measurement of interfacial tensions. Phys. Rev. Lett. 72, 2298-2301.

3. Foty, R., C. Pfleger, G. Forgacs and M. Steinberg 1996. Surface tensions of embryonic tissues predict their mutual envelopment behavior. Development. 122, 1611-1620.

4. Forgacs, G., R.A. Foty, Y. Shafrir and M.S. Steinberg 1998. Viscoelastic properties of living embryonic tissues: A quantitative study. Biophys. J. 74, 2227-2234.

5. Jia, D., D. Dajusta and R.A. Foty 2007. Tissue surface tensions guide in vitro self-assembly of rodent pancreatic islet cells. Developmental Dynamics. 236, 2039.

6. Foty, R. A., S.A. Corbett, J.E. Schwarzbauer and M.S. Steinberg 1998. Dexamethasone up-regulates cadherin expression and cohesion of HT-1080 human fibrosarcoma cells. Cancer Res. 58, 3586-3589.

7. Foty, R. A. and M.S. Steinberg 1997. Measurement of tumor cell cohesion and suppression of invasion by E- or P-cadherin. Cancer Res. 57, 5033-5036.

8. Brian S. Winters, Scott R. Shepard,Ramsey A.Foty, 2005. Biophysical measurement of brain tumor cohesion. International Journal of Cancer. 114, 371-379.

9. Steinberg, M. S. 2007. Differential adhesion in morphogenesis: A modern view. Current Opinion in Genetics & Development. 17, 281-286.

10. Foty, R. A. and M.S. Steinberg 2005. The differential adhesion hypothesis: A direct evaluation. Developmental Biology. 278, 255-263.

11. Gates, Julie and Peifer, Mark 2005. Can 1000 reviews be wrong? actin, α-catenin, and adherens junctions. Cell. 123, 769-772.

12. Niessen, C. M. and B.M. Gumbiner 2002. Cadherin-mediated cell sorting not determined by binding or adhesion specificity. J. Cell Biol. 156, 389-400.

13. Brodland, G. 2002. The differential interfacial tension hypothesis (DITH): A comprehensive theory for the self-rearrangement of embryonic cells and tissues. Journal of Biomechanical Engineering. 124, 188-197.

14. Brodland, G. 2004. Computational modeling of cell sorting, tissue engulfment, and related phenomena: A review. Appl. Mech. Rev. 57, 47-76.

15. Viens, D. and G.W. Brodland 2007. A three-dimensional finite element model for the mechanics of cell-cell interactions. J. Biomech. Eng. 129, 651-657.

16. Beloussov, LV Grabovsky, VI 2006. Morphomechanics: Goals, basic experiments and models. International Journal of Developmental Biology. 50, 89-91.

17. Pérez-Pomares, J. M. and R.A. Foty 2006. Tissue fusion and cell sorting in embryonic development and disease: Biomedical implications. Bioessays. 28, 809-821.

18. Tepass, U., D. Godt and R. Winklbauer 2002. Cell sorting in animal development: Signalling and adhesive mechanisms in the formation of tissue boundaries. Current Opinion in Genetics & Development. 12, 572-582.

19. Byrne, H. M. 1997. The importance of intercellular adhesion in the development of carcinomas. Math Med Biol. 14, 305-323.

20. Foty, RA and Steinberg, MS 2004. Cadherin-mediated cell-cell adhesion and tissue segregation in relation to malignancy. International Journal of Developmental Biology. 48, 397-409.

21. Guiot, C., P. Delsanto and T. Deisboeck 2007. Morphological instability and cancer invasion: A 'splashing water drop' analogy. Theoretical Biology and Medical Modelling. 4, 4.

22. Kelleher, F., D. Fennelly and M. Rafferty 2006. Common critical pathways in embryogenesis and cancer. Acta Oncol. 45, 375-378.

23. Jakab, K., A. Neagu, V. Mironov, R.R. Markwald and G. Forgacs 2004. Engineering biological structures of prescribed shape using self-assembling multicellular systems. PNAS. 101, 2864-2869.

24. Napolitano, A. P., P. Chai, D.M. Dean and J.R. Morgan 2007. Dynamics of the self-assembly of complex cellular aggregates on micromolded nonadhesive hydrogels. Tissue Eng. 13, 2087-2094.

25. D R Nisbet, S Pattanawong, N E Ritchie, W Shen, D I Finkelstein,M K Horne and J S Forsythe 2007. Interaction of embryonic cortical neurons on nanofibrous scaffolds for neural tissue engineering. Journal of Neural Engineering. 4, 35-41.

26. Fabrizio Gelain, Akihiro Horii,Shuguang Zhang, 2007. Designer self-assembling peptide scaffolds for 3-D tissue cell cultures and regenerative medicine. Macromolecular Bioscience. 7, 544-551.

27. Marler, J. J., J. Upton, R. Langer and J.P. Vacanti 1998. Transplantation of cells in matrices for tissue regeneration. Advanced Drug Delivery Reviews. 33, 165.

28. Mironov, V., G. Prestwich and G. Forgacs 2007. Bioprinting living structures. Journal of Materials Chemistry. 17, 2054.

29. Armstrong, N. J., K.J. Painter and J.A. Sherratt 2006. A continuum approach to modeling cell–cell adhesion. Journal of Theoretical Biology. 243, 98-113.

30. Brodland, G. 2003. New information from cell aggregate compression tests and its implications for theories of cell sorting. Biorheology. 40, 273-277.

31. Cuvelier, D., M. Théry, Y. Chu, S. Dufour, J. Thiéry, M. Bornens, P. Nassoy and L. Mahadevan 2007. The universal dynamics of cell spreading. Current Biology. In Press, Corrected Proof.

32. Turner, S. 2005. Using cell potential energy to model the dynamics of adhesive biological cells. Phys Rev E Stat Nonlin Soft Matter Phys. 71, 041903.

33. Hardin, J. and T. Walston 2004. Models of morphogenesis: The mechanisms and mechanics of cell rearrangement. Current Opinion in Genetics & Development. 14, 399-406.

34. Friedl, P. 2004. Prespecification and plasticity: Shifting mechanisms of cell migration. Current Opinion in Cell Biology. 16, 14-23.

35. Jason G. Homsy, Heinrich Jasper, Xomalin G. Peralta, Hai Wu, Daniel P. Kiehart,Dirk Bohmann, 2006. JNK signaling coordinates integrin and actin functions during *drosophila* embryogenesis. Developmental Dynamics. 235, 427-434.

36. Hegedus, B., F. Marga, k. jakab, K. Sharpe-Timms and G. Forgacs 2006. The interplay of cell-cell and cell-matrix interactions in the invasive properties of brain tumors. Biophys. J., 77834.

37. Neagu, A., K. Jakab, R. Jamison and G. Forgacs 2005. Role of physical mechanisms in biological self-organization. Phys. Rev. Lett., 17804.

38. Carter, G. W. 2005. Inferring network interactions within a cell. Brief Bioinform. 6, 380-389.

39. Beysens, D. A., G. Forgacs and J.A. Glazier 2000. Cell sorting is analogous to phase ordering in fluids. PNAS. 97, 9467-9471.

40. Steinberg, M. S. and S.F. Gilbert 2004. Townes and holtfreter (1955): Directed movements and selective adhesion of embryonic amphibian cells. Journal of Experimental Zoology Part A: Comparative Experimental Biology. 301A, 701-706.

41. Trinkaus, JP and Groves, PW 1955. Differentiation in culture of mixed aggregates of dissociated tissue cells. PNAS. 41, 787-795.

42. Moscana, A. 1957. The development in vitro of chimeric aggregates of dissociated embryonic chick and mouse cells. PNAS. 43, 184-194.

43. Steinberg, M. 1963. Reconstruction of tissues by dissociated cells. some morphogenetic tissue movements and the sorting out of embryonic cells may have a common explanation. Science., 401-408.

44. Wiseman, L. L. 1977. Can the differential adhesion hypothesis explain how an aggregate of strongly cohesive cells can be penetrated by more weakly cohesive cells? Developmental Biology. 58, 204-211.

45. Harris, A. K. 1976. Is cell sorting caused by differences in the work of intercellular adhesion? A critique of the Steinberg Hypothesis. Journal of Theoretical Biology. 61, 267-285.

46. Mège, R., J. Gavard and M. Lambert 2006. Regulation of cell–cell junctions by the cytoskeleton. Current Opinion in Cell Biology. 18, 541-548.

47. Sheetz, M. P. 2001. Cell control by membrane-cytoskeleton adhesion. Nat. Rev. Mol. Cell Biol. 2, 392-396.

48. Chen, H. and G. Brodland 2000. Cell-level finite element studies of viscous cells in planar aggregates. Journal of Biomechanical Engineering. 122, 394-401.

49. Duguay, D., R.A. Foty and M.S. Steinberg 2003. Cadherin-mediated cell adhesion and tissue segregation: Qualitative and quantitative determinants. Dev. Biol. 253, 309-323.

50. Freshney, R. I. 2000. Culture of Animal Cells: A Manual of Basic Technique. Wiley-Liss, Toronto, Ontario, Canada.

51. Jaroszeski M. J., Gilbert R. and Heller R, 1994. Detection and Quantitation of Cell-Cell Electrofusion Products by Flow Cytometry. Analytical Biochemistry. 216, 2, 271-275.

52. Jae Oh, Duk, Martinez, Alexander R. , Lee, Gyun Min, O. Palsson, Bernhard, Francis, Karl, 2000. Intercellular adhesion can be visualized using fluorescently labeled fibrosarcoma HT1080 cells cocultured with hematopoietic cell lines or CD34+ enriched human mobilized peripheral blood cells. Cytometry, 40,2, 119-125.

Appendix A: Force-time Curves

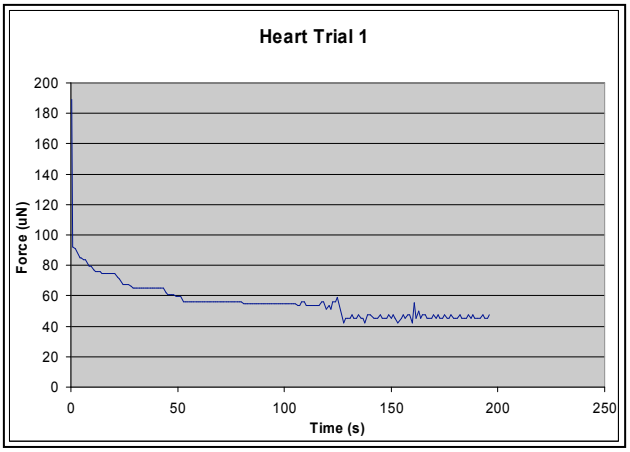

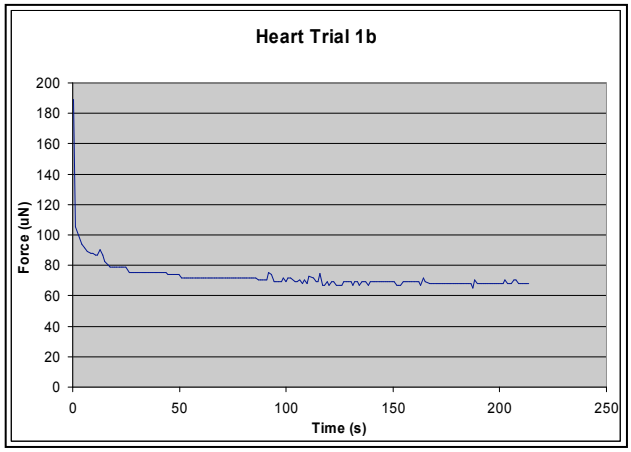

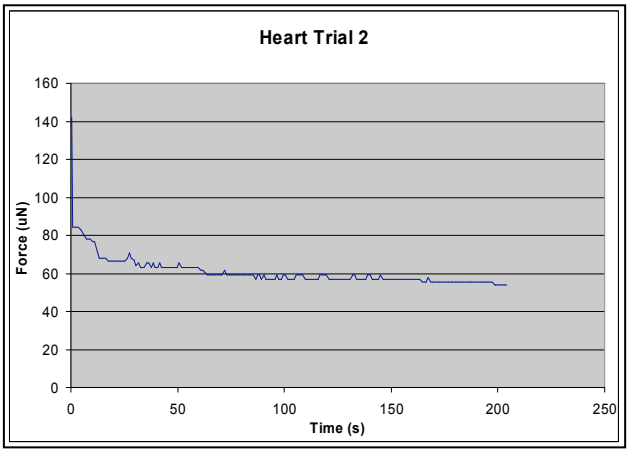

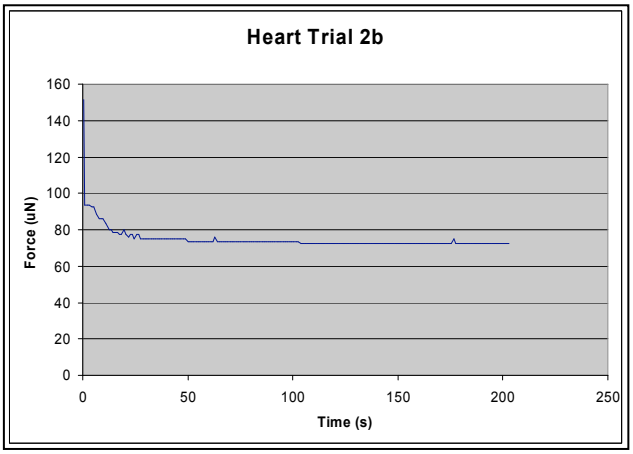

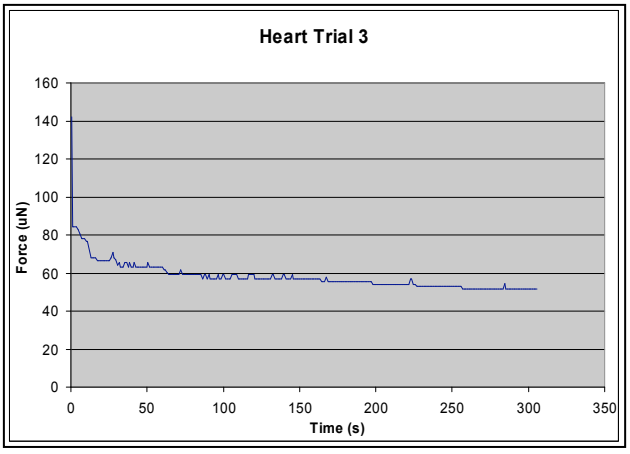

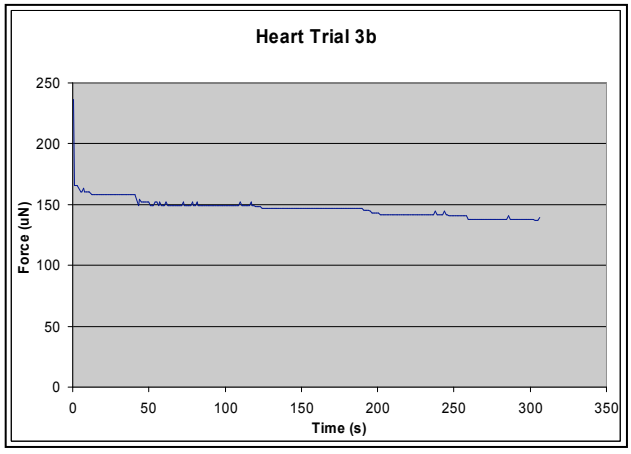

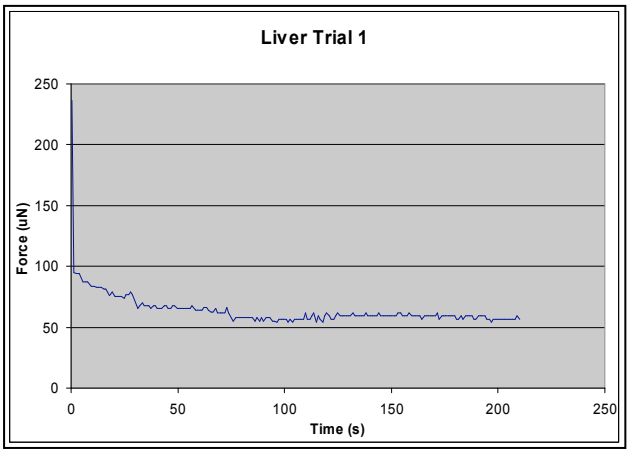
Liver Trial 1
Force (uN)
Time (s)
0
50
100
150
200
250

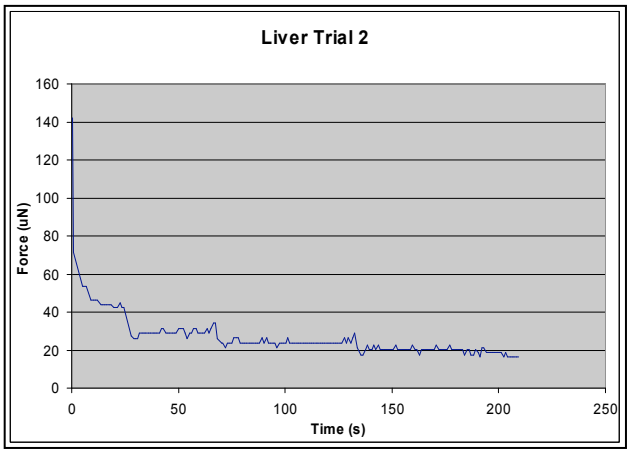
Liver Trial 2
Force (uN)
Time (s)
0
20
40
60
80
100
120
140
160

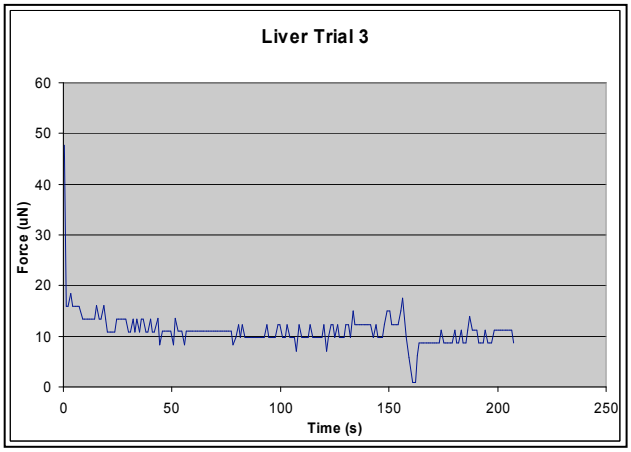
Liver Trial 3
Force (uN)
Time (s)
0
10
20
30
40
50
60

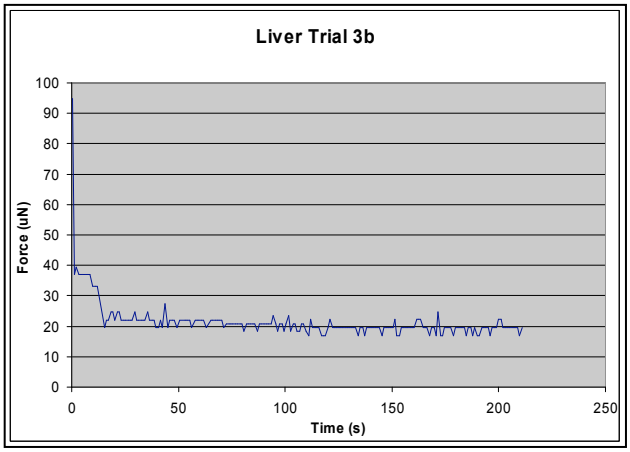
Liver Trial 3b
Force (uN)
Time (s)
0
10
20
30
40
50
60
70
80
90
100

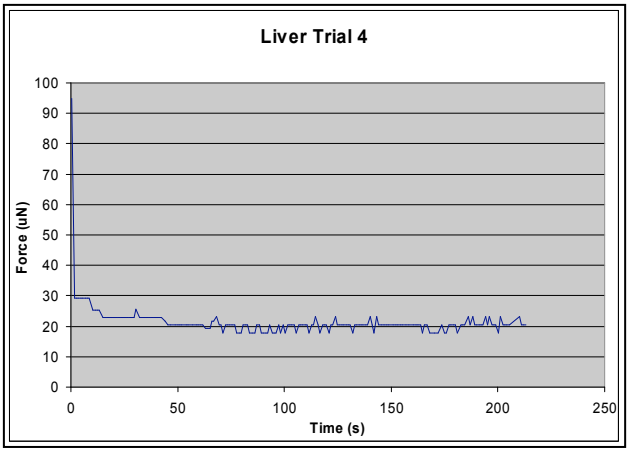
Liver Trial 4
Force (uN)
Time (s)
0
10
20
30
40
50
60
70
80
90
100

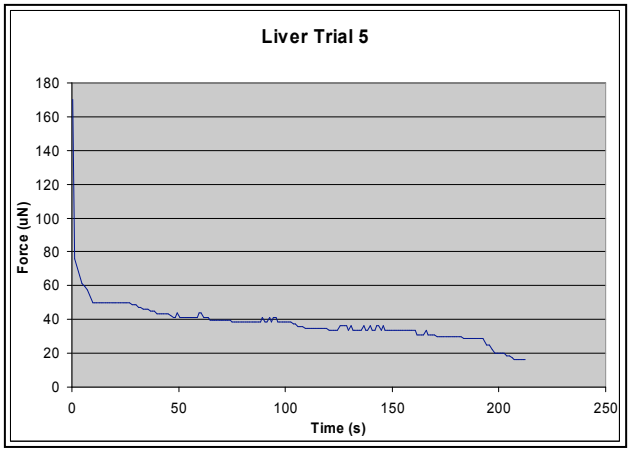
Liver Trial 5
Force (uN)
Time (s)
0
20
40
60
80
100
120
140
160
180

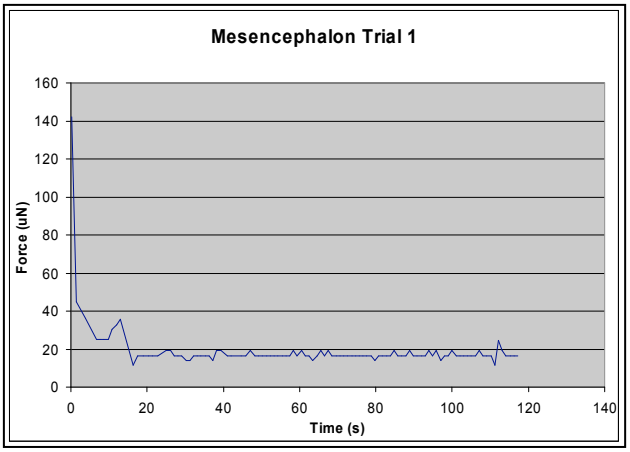
Mesencephalon Trial 1
Force (uN)
Time (s)
0
20
40
60
80
100
120
140
160

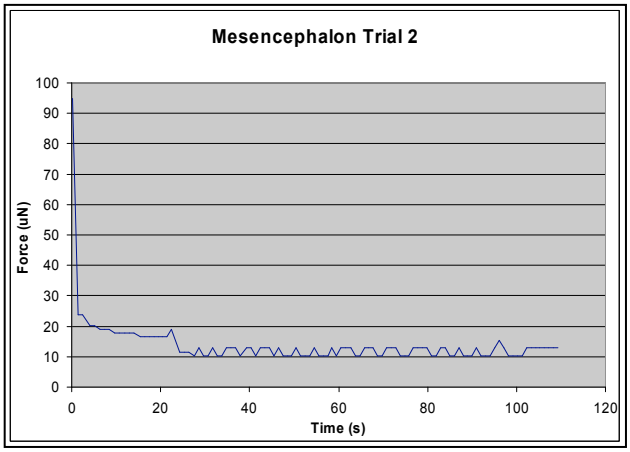
Mesencephalon Trial 2
Force (uN)
Time (s)
0
10
20
30
40
50
60
70
80
90
100
120

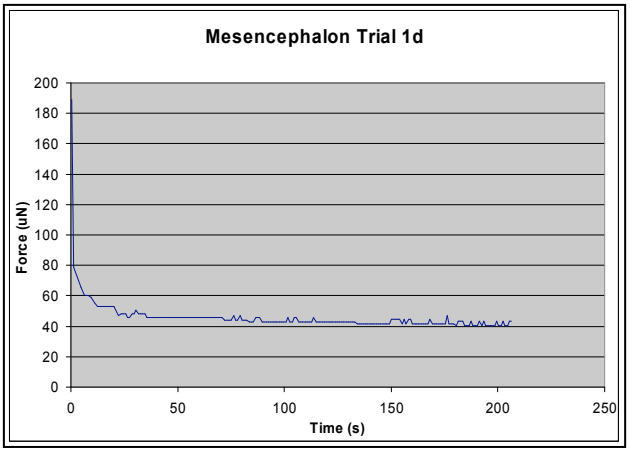
Mesencephalon Trial 1d
Force (uN)
Time (s)
0
20
40
60
80
100
120
140
160
180
200
250

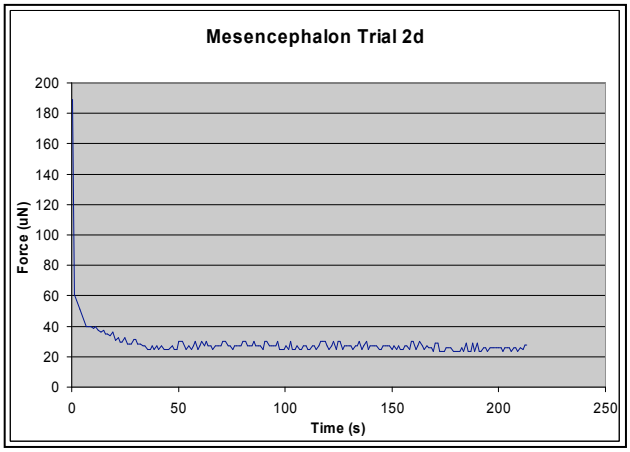
Mesencephalon Trial 2d
Force (uN)
Time (s)
0
20
40
60
80
100
120
140
160
180
200
250

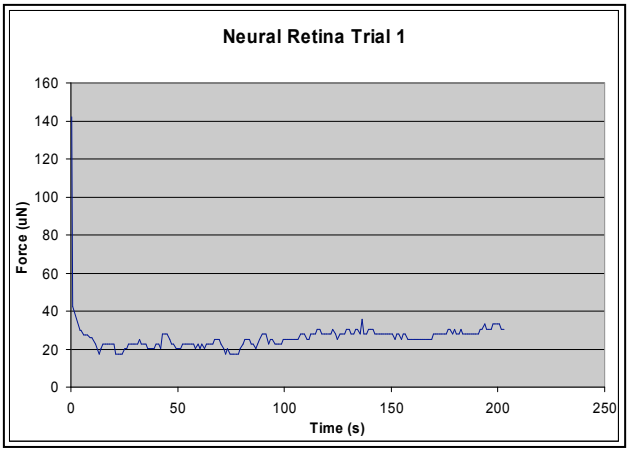
Neural Retina Trial 1
Force (uN)
Time (s)
0
20
40
60
80
100
120
140
160
0
50
100
150
200
250

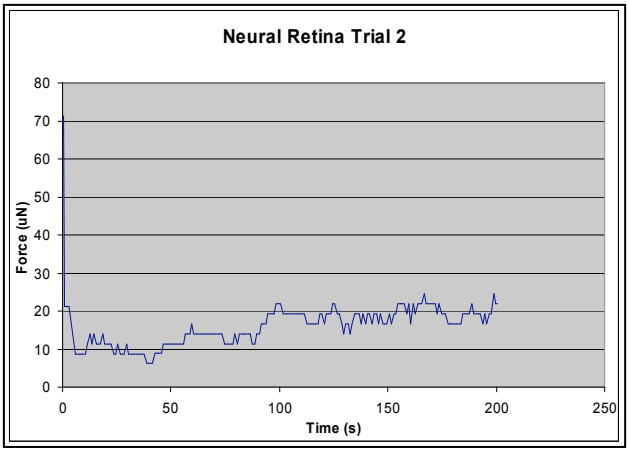
Neural Retina Trial 2
Force (uN)
Time (s)
0
10
20
30
40
50
60
70
80
0
50
100
150
200
250

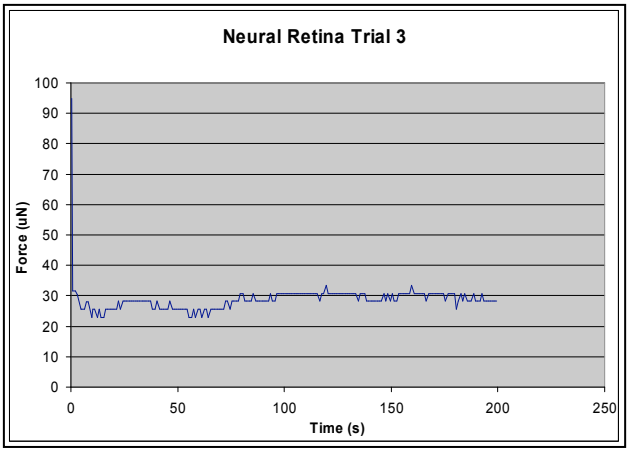
Neural Retina Trial 3
Force (uN)
Time (s)
0
10
20
30
40
50
60
70
80
90
100
0
50
100
150
200
250

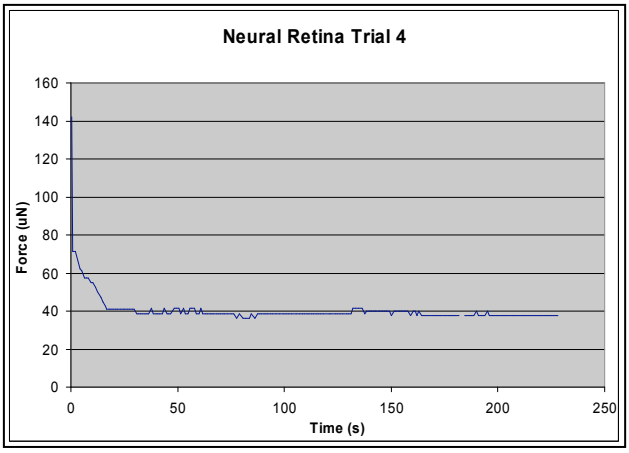
Neural Retina Trial 4
Force (uN)
Time (s)
0
20
40
60
80
100
120
140
160
0
50
100
150
200
250

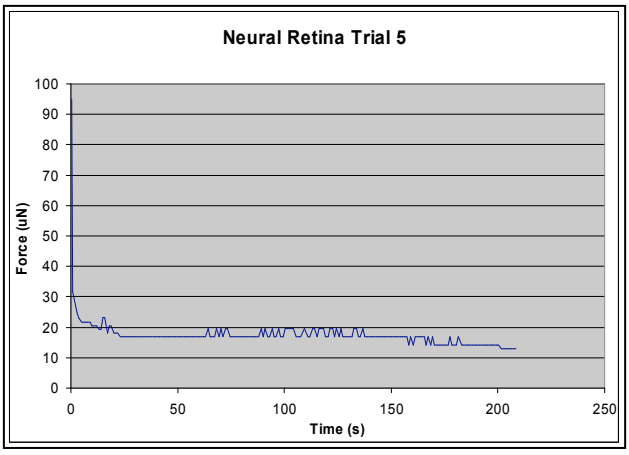
Neural Retina Trial 5
Force (uN)
Time (s)
0
10
20
30
40
50
60
70
80
90
100
0
50
100
150
200
250